Weidner, A.; Pyczak, F.; Biermann, H.:

Scanning and transmission electron microscopy investigations of defect arrangements in a two-phase Gamma-TiAl alloy

In: Materials Science and Engineering A (2013) Elsevier

DOI: 10.1016/j.msea.2013.01.078

Scanning and transmission electron microscopy investigations of defect arrangements in a two-phase γ-TiAl alloy

A. Weidner[a*)], F. Pyczak[b)], H. Biermann[a)]

[a)] Institute of Materials Engineering, Technische Universität Bergakademie Freiberg, Gustav-Zeuner-Str. 5, 09596 Freiberg, Germany

[b)] Institute of Materials Research, Department of Metal Physics, Helmholtz-Zentrum Geesthacht, Max-Planck-Str. 1, 21502 Geesthacht, Germany

Abstract

Different methods of scanning and transmission electron microscopy (SEM, TEM) were applied on a γ-TiAl alloy TNB-V5 after a thermo-mechanical fatigue test. Electron channelling contrast imaging (ECCI) and electron backscattered diffraction were carried out on bulk specimen. In addition, ECCI and scanning transmission electron microscopy in the SEM were carried out on a TEM-foil in the electron opaque and the electron transparent region, respectively. The investigations were completed by transmission electron microscopy in form of standard bright field imaging as well as by taking corresponding diffraction patterns. The results demonstrate in an impressive way that the ECCI technique applied in scanning electron microscope can successfully supplement or in some cases replace imaging of dislocation arrangements in TEM.

Keywords

Titanium aluminide alloys, electron channelling contrast imaging, transmission electron microscopy, EBSD

1. Introduction

The commonly used technique for the investigation of the deformation microstructure on the nano/micro scale is transmission electron microscopy (TEM). It allows the investigation of lattice defects like dislocations, stacking faults and/or micro twins in individual grains. In addition, information on the crystallographic orientation of the investigated grain is available. However, the investigated number of grains is very restricted due to the limited size of the electron transparent region. In this context, advanced techniques applied in scanning electron microscope help to overcome these restrictions. Complementary to TEM, the combination of electron channelling contrast imaging (ECCI) technique and electron backscattered diffraction (EBSD) in a high-resolution field emission SEM (HR-FE-SEM) can be applied to bulk specimens.

The ECCI technique can be used for the characterization of microstructures after plastic deformation, e.g. [1-5], because it allows the visualization of condensed dislocation arrangements near the surface of bulk specimens, e.g. dislocation walls/cells after fatigue [1, 6-9]. Even the imaging of individual dislocations [5, 10-12] is possible under defined diffraction conditions. The main advantages of the ECCI technique compared to transmission electron microscopy (TEM) are that (i) images can be taken from bulk specimens making this technique very attractive for the examination of defects during in-situ deformation and (ii) much better statistics on the dislocation arrangements can be obtained. The application of

[*] Corresponding author: Tel.: +49-3731-39 2124, Fax: +49-3731-39 3703,
email-address: weidner@ww.tu-freiberg.de

the ECCI technique in combination with EBSD measurements in a SEM gives a great potential for investigating and improving the knowledge on the underlying deformation mechanisms and to clarify the deformation behaviour of metals, e.g. tensile and cyclic deformation of TRIP steels [11-12]. ECCI performed under exact Bragg condition reveals excellent contrast for investigations of dislocations [13]. Defects like individual dislocations lead to a local lattice distortion and as a consequence the Bragg condition is locally not fulfilled. Therefore, individual dislocations will appear as bright lines in a dark matrix. Applying an inverted signal of BSE contrast, inverted ECC images are obtained, where dislocations appear as dark lines in a bright matrix in analogy to TEM bright field micrographs.

Titanium aluminide (γ-TiAl) alloys with their low density (3.7 – 4.7 g/cm³), high melting temperature (in the range of 1700 K) and good oxidation resistance are attractive candidates for high temperature applications in the automotive and aerospace industry and have been in focus of scientific interest since many years [14]. Most γ-TiAl alloys are based on a two phase microstructure which contains the tetragonal γ-TiAl phase with a $L1_0$-structure and the hexagonal α_2-Ti_3Al phase with a DO_{19}-structure. Four different types of microstructures formed by these two phases are known [15]: near gamma (NG), duplex (DP), nearly lamellar (NL) and fully lamellar (FL). γ - TiAl alloys of the 3rd generation containing higher concentrations of Nb (5 - 10 %) exhibit a high strength combined with acceptable room temperature ductility and damage tolerance due to their fine-grained microstructure.

The deformation behaviour of the γ-phase is determined by dislocation glide processes in the $L1_0$-structure [16]. Dislocation glide is activated on {111} γ planes along the close packed directions <110>. Both, ordinary dislocations of Burgers vector b = ½ <110] as well as super dislocations with the Burgers vector b = ½ <112] or b = <101] can occur. A second possible deformation mechanism is the formation of deformation twins along 1/6 <11-2] on the {111} γ plane. The complex dissociation in partial dislocations forming planar defects like antiphase boundaries or stacking faults was observed for super dislocations of type ½ <112] and <101] [17]. A dissociation in partial dislocations is not reported for ordinary dislocations of type ½ <110]. The deformation behaviour of two phase γ-TiAl alloys up to high temperatures (973 K) is determined by the easy activation of <110] dislocation glide and mechanical twinning [17]. The motion of super dislocations is suppressed in that temperature regime [18]. Henaff et al. [19] showed that in Ti-48Al-2Nb-2Cr specimens which experienced LCF at temperatures as low as 723 K the dislocation structure consists of ordinary dislocations which showed signs of recovery and climb processes. Corresponding features are also remnant dislocation loops, which were reported by Jouiad et al. [20] in the same alloy for LCF at 1023 K. Also Appel et al. [21] found climbed and cross slipped dislocation segments in a Ti-45Al-8Nb-0.2C alloy after LCF at 823 K. But, besides these features also dense dislocation walls are reported by Appel et al. [22] in the same alloy also at 823 K.

The main objective of the present paper is to demonstrate the application of the ECCI technique to study the dislocation arrangements in comparison with TEM investigations and STEM investigations in a SEM. For these investigations the γ-TiAl alloy (TNB-V5) with a duplex microstructure after a thermo-mechanical fatigue test [23] was chosen.

2. Material and deformation tests

Investigations of the microstructure after a thermo-mechanical fatigue test were carried out on the γ-TiAl alloy TNB-V5. The material with the nominal chemical composition Ti-45Al-5Nb-0.2C-0.2B (at %) was produced by Plansee AG (Reutte). The investigated material showed a so-called duplex structure with 40 % of globular γ-TiAl grains and 60 % of lamellar colonies with γ/α_2-lamellae. The mean grain size of globular γ-TiAl grains is about 2 to 4 µm, the size of lamellar colonies ranges from 5 to 25 µm and the inter lamellar spacing varies from 50 to 500 nm. Figure 1 shows an overview of the duplex microstructure (SEM micrograph, backscattered electron contrast).

Insert Figure 1 about here

The TMF test was performed on a compact cylindrical specimen with a gauge length of 19 mm and a gauge diameter of 7.0 mm. The specimen surface was electrolytically polished. The TMF test was carried out on a servo hydraulic testing system under total-strain control mode with a mechanical strain amplitude of $\varepsilon_{a,mech} = 5.75 \times 10^{-3}$ and a strain rate of 9.20×10^{-5} s^{-1} [23]. The applied temperature interval was $673\ K \leq T \leq 923\ K$. The TMF temperature–strain cycles were applied in-phase (IP) and both, the mechanical strain cycles and the temperature cycles had a triangular shape. The specimen was heated with a high frequency induction heater at a heating rate of 2 K/s. Axial temperature deviations within the gauge length were below ±5 K [24]. The corresponding cyclic deformation curve and stress-strain hysteresis loops are shown in Figure 2. Initially, the stress amplitude slightly decreases reaching saturation at about 10 cycles. Furthermore, it becomes evident from the stress-strain hysteresis loops that a compressive mean stress is present from the beginning of deformation. This compressive mean stress is increasing with ongoing deformation as a result of a decreasing upper stress [25].

Insert Figure 2 about here

After failure at $N_f = 742$ cycles, the specimen was cut parallel to the loading axis. One half of the specimen was prepared for SEM investigations. From the other part TEM foils were prepared. EBSD and ECCI investigations on the bulk specimens were performed in the plane parallel to the loading axis using field emission scanning electron microscopes (LEO 1530 from ZEISS, MIRA3 XMU from TESCAN). The OIM software from TSL was used for EBSD measurements under a specimen tilt of 70° and an acceleration voltage of 20 kV. The ECCI investigations were performed using a retractable four-quadrant backscattered electron detector allowing working distances of 8 mm. The MIRA 3 XMU is working with a single aperture of 10 µm. The beam current can be adjusted continuously up to 100 nA. Information about the effective probe current and the resulting spot diameter on the specimen surface are always available due to the real time “in-flight beam tracing” technology. ECCI investigations were performed at an acceleration voltage of 20 kV using a 10 µm aperture and a probe current < 2 nA. The lattice parameters, which were used for the phase identification by EBSD, are summarized in Tab. 1.

Insert Table 1 about here

Normally, the best surface state of specimens for ECCI investigations is obtained by electrolytic polishing. However, in multiphase materials like the present TiAl-TNB-V5 alloy electrolytic polishing leads to a pronounced surface relief. A method to avoid such a pronounced surface relief is vibration polishing (Buehler) for about 24 hours. The removal of material is very gentle. Therefore, by this method a very smooth and deformation free surface is obtained.

The specimens for TEM investigations were prepared perpendicular to the external load axis. A cylinder with a diameter of 3 mm was machined by spark erosion. Discs with a thickness of approximately 300 µm were cut and ground up to a final thickness of 150 µm. The discs were electrolytically thinned to electron transparency using a mixture of methanol (60%), butanol (34%) and perchloric acid (6%) as agent at a temperature of 243 K and a voltage of 25 V. The TEM investigations were performed in a Philips CM200 with an acceleration voltage of 200 kV.

Additionally, the TEM foils were investigated in the FE-SEM (MIRA3) applying ECCI as well as using a transmission electron (TE) detector. The TE detector can be used in bright-field and dark-field mode. The TE detector was mounted directly on the SEM specimen stage. The working distance is 3 mm. Best imaging conditions were obtained at an acceleration voltage of 30 kV and a beam current of 100 pA.

3. Results and discussion

3.1 SEM investigation – EBSD and ECCI

Figure 3 shows two examples of SEM investigations on the TiAl specimen. Inverted ECCI images (a,d) are shown together with EBSD grain orientation maps (b,e) and EBSD phase maps (c,f) of two areas of interest. The grain orientation maps are coloured according to the colour code of the stereographic standard triangle of the surface normal direction. In the phase maps the green colour represents γ-TiAl and the red colour α_2-Ti_3Al. In the lamellar regions alternating lamellae of γ-TiAl and α_2-Ti_3Al were detected if the α_2-Ti_3Al lamellae are thick enough. Two different areas of interest were chosen in order to demonstrate the great variance of microstructural features, which becomes evident from the ECCI overview images. Even without additional tilting/rotating of the specimen, several individual grains are in perfect imaging conditions for visualization of microstructural details like twins or dislocations. Already from the overview ECCI images of the whole areas of interest it is possible to distinguish several different “internal” structures inside individual γ-TiAl grains or in the lamellar regions. Four individual grains were labelled in Figures 3a and d, respectively. For these grains inverted ECCI images were taken at higher magnification in order to illustrate the microstructural features developed during thermo-mechanical fatigue. These high-resolution ECCI images are summarized in Figure 5 for area I and in Figure 6 for area II. The crystallographic orientations of these individual grains are summarized in Table 2.

The inverted ECCI micrographs in Figure 4 show the internal structure both in γ-TiAl lamellae in the lamellar regions (a, c) as well as in the globular γ-TiAl grains. In all cases the specimen was not tilted and the grain orientation was used as it is for the ECCI investigations. The crystallographic orientation of these grains can be obtained from the EBSD grain orientation map in Fig. 3b and 3e and Table 2, respectively. In the lamellar regions the dark areas correspond to the hexagonal α_2-Ti_3Al phase. In all four grains individual dislocations can be

clearly detected. Figure 4b shows in addition mechanically formed micro twins (marked by arrows).

Insert Figure 3 about here

Insert Figure 4 about here

In addition, between these micro twins individual dislocations are visible running along different directions. In Figure 4c a slightly disoriented subgrain structure becomes visible. Figure 4d represents an example for elongated individual dislocations, which seem to be pinned. Based on alloy composition the black particles which frequently pin dislocations (indicated by arrows) could either be borides or carbides. No attempt to identify them e.g. by diffraction in TEM was undertaken, while they are too small for EBSD/EDX analysis in SEM.

Figure 5 shows additional microstructural features. Figure 5a contains at least 4 different features: (i) long individual dislocations, (ii) dislocation tangles, (iii) micro twins and (iv) stacking fault contrast originated by a micro twin (marked by arrows). In Figure 5b two small γ-TiAl grains with nearly the same surface normal direction are shown. However, the left grain contains dislocation tangles, whereas in the right grain micro twins (arrows) and elongated individual dislocations between these micro twins are visible. The formation of micro twins is well illustrated in Figure 5c (arrows). Moreover, the formation of a subgrain structure containing several individual dislocations is visible, too. Figure 5d illustrates again a dislocation arrangement consisting of elongated dislocations, which are pinned at their ends (arrows) as well as of dislocation tangles.

Insert Figure 5 about here

3.2 SEM investigation on a TEM-foil

A TEM foil from the same deformation state was studied in an HR-FE-SEM. Both, the electron transparent region as well as the electron opaque area were investigated by application of two different techniques. First, the bright-field transmission electron detector was used. Figure 6 shows dislocation arrangements in globular (a, b) and lamellar (c) γ-TiAl areas.

Figure 6a is comparable to Fig. 4b and Fig. 5a-c. It shows narrow bands running through the whole grain which are most probably twins. Also long dislocation segments inclined to the micro twins are visible. Some of the segments are pinned by obstacles resulting in the bow-out structure. Also debris and small dipole loops become visible. Even in very thin γ-TiAl areas between α_2-Ti_3Al lamellae dislocation arrangements can be imaged. Unfortunately, it is impossible to obtain directly information on the crystallographic orientation of the investigated grains. For this purpose, the detour via EBSD measurements on the TEM foil is necessary. Moreover, detailed burgers vector analysis seems to be difficult by this technique because the possibility for tilting the specimen is very limited due to the low working distance of 3 mm. The area for investigations is limited to electron transparent regions like for TEM investigations. However, it should be noted that TE images in the SEM were obtained at an acceleration voltage of 30 kV in contrast to the acceleration voltages between 80 and 300 kV conventional TEMs are working at.

Insert Figure 6 about here

The rather limited statistics of grains accessible for investigation in the electron transparent area of a TEM foil can be improved significantly by applying the ECCI technique to the electron opaque areas of TEM foils or on bulk specimens. Figures 7 and 8 show dislocation arrangements in globular γ-TiAl grains of a TEM foil and a bulk specimen, respectively. Micro twins, long screw dislocation segments, dislocation segments pinned by obstacles, debris and dislocation loops are visible in ECCI contrast. Even in the narrow γ-phase lamellae with a typical thickness < 500 nm individual dislocations and micro twins are detectable (Fig. 8d). γ-phase lamellae show a fragmentation either by micro twins or by specific dislocation arrangements. The main advantage applying ECCI on bulk specimens, i.e. high grain statistic, becomes evident from the following fact. Although all micrographs were taken on the specimen just as mounted on the SEM stage without knowing the individual crystallographic orientation, a large number of grains are in good diffraction conditions for imaging dislocation arrangements without additional tilting and rotating the specimen. Therefore, ECCI on bulk specimens is a good way to obtain a statistically sound overview of the deformation microstructure, especially dislocations and twins. Nevertheless, for an exact description of the crystallographic nature of dislocation arrangements information about the exact diffraction conditions is necessary. Performing EBSD measurements before or after the ECCI investigation on the same area can provide the crystallographic orientation of each individual investigated grain. By this, the exact diffraction conditions can be calculated for certain types of dislocations.

Insert Figure 7 about here

Insert Figure 8 about here

3.3 TEM investigations

In order to verify the information of the SEM studies and to get more detailed information on the type of dislocations activated during the thermo-mechanical fatigue test and other microstructural features additional TEM investigations were performed. In a γ-grain oriented close to the [1-10] zone axis micrographs were recorded under two beam conditions using the (111), (220), (11-1) and (002) reflections. Figure 8 shows an overview of the γ-grain under investigation with the indexed diffraction pattern of the γ-phase as an inset. The micrograph in Figure 9a was recorded using a (111) reflection two beam condition and shows a number of deformation twins stretching over the whole grain while long dislocation segments are found which lie inclined to these twins. All dislocations are out of contrast when using a [002] two beam condition. This is an indication that no super dislocations are present in this grain. Figure 9b shows a part of this γ-grain in higher magnification using the same imaging conditions. By comparing the trace of the (11-1) plane which is marked by a dashed line with the direction of the twins it is obvious that the deformation twins lie in this crystallographic plane. They do not appear as lines because the foil was slightly tilted away from the [1-10] zone axis for recording Figure 9b under the [111] two beam condition. The dislocation segments are mainly oriented parallel to the [110] direction which is indicated by an arrow. No complete Burgers vector analysis was performed, but as the majority of dislocations are out of contrast using the [002] diffraction vector and show contrast using the [110] diffraction vector they are probably ordinary dislocations of the Burgers vector $b = \pm \frac{1}{2}$ [110] type. Accordingly, the majority of dislocation segments are parallel to [110] and hence

of screw character. Some dislocation segments are bowed out. The observed micro twins and the dislocation arrangement between these micro twins are comparable to those imaged applying the ECCI technique on a bulk specimen as shown in Figure 4d.

Insert Figure 9 about here

From Figure 9b it is clear that these bowed-out sections of dislocations are pinned by small obstacles. In addition, in Figure 8b also other features like debris and remnant dislocation loops are visible. These features are normally associated in literature [16] with excess vacancies which act as dislocation obstacles, remnant dislocation dipoles developing at jogs and by-products of dislocation climb and multiplication processes. As the present study concentrates on comparison of different microscopy methods and not on deformation structures in TiAl-alloys the reader is kindly referred to the literature for more details. Nevertheless, it is noteworthy that similar features are reported for TiAl specimens after LCF in the 723 – 823 K regime [19-21].

Another feature of the deformation structure is revealed in Figure 10a. Here, a stacking fault is observed using the (002) reflection. This stacking fault starts at the boundary of a deformation twin and is probably associated with slip transfer through this twin boundary. It is not a single stacking fault but a stacking fault ribbon generated by the successive glide of a number of partial dislocations. Also in the lamellar region of the microstructure deformation in the γ-phase is mainly associated with dislocation movement. Figure 10b shows long dislocation segments in a lamellar γ-TiAl microstructure running between Ti_3Al lamellae. Overall the features pictured by TEM in this specimen correspond very well with the micrographs obtained by ECCI and STEM in the SEM in the same TMF specimen.

Insert Figure 10 about here

4. Summary

The present investigations showed a comparison between different advanced techniques of scanning electron microscopy and transmission electron microscopy.

Investigations on the microstructure of the γ-TiAl alloy TNB-V5 after thermo-mechanical fatigue tests were performed by scanning and transmission electron microscopy. The main goal of the presented results was to demonstrate that the application of the ECCI technique on bulk specimens as well as on TEM-foils is a very powerful method to study the arrangements of deformation induced defects like micro twins, stacking faults and/or regular dislocations. The shown microstructural features are already well known from the literature and are the same as in the isothermal LCF regime.

The results obtained from combined EBSD and ECCI investigations on the bulk specimen demonstrate vividly that dislocation structures can be visualized both in the globular γ-TiAl grains as well as in the γ-TiAl lamellae of the lamellar regions (alternating γ-TiAl and α_2-Ti_3Al lamellae). The visualized defect types and/or arrangements by application of ECCI technique are in resolution comparable to those obtained from STEM or TEM investigations. It becomes evident from the presented ECCI investigations that on a bulk specimen the investigation of dislocation and/or defect arrangements can be performed with a reasonable good statistics. In combination with EBSD it is even possible to investigate the influence of crystallographic orientation with a reasonable time exposure.

Acknowledgment

Dr. M. Roth is gratefully acknowledged for the providing the TiAl specimens after thermo-mechanical fatigue. The authors thank Ms. A. Müller and Ms. K. Zuber from the Institute of Materials Science for careful preparation of TiAl specimens for EBSD and ECCI investigations.

References

[1] R. Zauter, F. Petry, M. Bayerlein, C. Sommer, H.-J. Christ, H. Mughrabi, Electron channelling contrast as a supplementary method for microstructural investigations in deformed metals, Phil. Mag. A 66 (1992) 425-436.

[2] A. J. Wilkinson, G. R. Anstis, J. T. Czernuszka, N.J. Long, P. B. Hirsch, Electron channelling contrast imaging of interfacial defects in strained silicon- germanium layers on silicon, Phil. Mag. A 68 (1993) 59-80.

[3] A. J. Wilkinson, P. B. Hirsch, Electron Diffraction Based Techniques in Scanning Electron Microscopy of Bulk Materials, Micron 28 (1997) 279-308.

[4] B. C. Ng, B. A. Simkin, M. A. Crimp, Application of the electron channeling contrast imaging technique to the study of dislocations associated with cracks in bulk specimens, Ultramicroscopy 75 (1998) 137145.

[5] I. Gutierrez-Urrutia, S. Zaefferer, D. Raabe, Electron channeling contrast imaging of twins and dislocations in twinning-induced plasticity steels under controlled diffraction conditions in a scanning electron microscope, Scripta Mater. 61 (2009) 737-740.

[6] B. A. Simkin, B. C. Ng, M. A. Crimp, Microscopy and Analysis (1999) 11.

[7] C. Buque, J. Bretschneider, A. Schwab, C. Holste, Mater. Sci. Eng. A 300 (2001) 254.

[8] Z. F. Zhang, Z. G. Wang, Z. M. Sun, Evolution and microstructural characterization of deformation bands in fatigued copper single crystals, Acta Mater. 49 (2001) 2875-2886.

[9] Y. Kaneko, K. Fukui, S. Hashimoto, Electron channeling contrast imaging of dislocation structures in fatigued austenitic stainless steels Mater. Sci. Eng. A 400-401 (2005) 413.

[10] A. Weidner, J. Man, W. Skrotzki, J. Polák, Slip Localization and Dislocation Structure at Early Stages of Fatigue Damage in Austenitic Stainless Steel (316L)Proceedings ICF12, Ottawa, (2009) CD-ROM fin00681.

[11] A. Weidner, S. Martin, V. Klemm, U. Martin, H. Biermann, Stacking faults in high-alloyed metastable austenitic cast steel observed by electron channelling contrast imaging, Scripta Mater. 64 (2011) 513–516.

[12] A. Weidner, A. Glage, L. Sperling, H. Biermann, Observation of stacking faults in a scanning electron microscope by electron channelling contrast imaging, Int. J. Mat. Res. (formerly Z. Metallkd.) 102 (2011)1-3.

[13] I. Gutierrez-Urrutia, D. Raabe, Dislocation density measurement by electron channelling contrast imaging in a scanning electron microscope, Scripta Mater. 66 (2012) 343-346.

[14] G.H. Meier, N. Birks, F.S.Pettit, R.A. Perkins, H.J. Grabke, Environmental behaviour of intermetallic materials, in: Strucutral Intermetallics, R. Darolia, j.J. Lewandowski, C.T. Liu, P.L. Martin, D.B. Miracle, M.V. Nathal (editors), TMS, Warrendale (1993) 861.

[15] Y.-W. Kim, D.M. Dimiduk, Progress in the understanding of gamma titanium aluminides. JOM 43 (1991) 40.

[16] F. Appel, R. Wagner, Microstructure and deformation of two-phase γ- titanium aluminides, Materials Science and Engineering R 22 (1998) 187-268.

[17] B.J. Inkson, C.J. Humphreys, High resolution electron microscopy observation of ½ <112> superdislocation in TiAl, Phil. Mag. Letters 71 (1995) 307.
[18] V.K. Vasudevan, M.A. Stucke, S.A. Court, H.L. Fraser, The influence of second phase Ti3Al on the deformation mechanisms in TiAl, Phil. Mag. Letters 59 (1989) 299.
[19] G. Henaff, A.-L. Gloanec, Fatigue properties of TiAl alloys, Intermetallics 13 (2005) 543–558.
[20] M. Jouiad, A.-L. Gloanec, M. Grange, G. Henaff, Cyclic deformation mechanisms in a cast gamma titanium aluminide alloy, Mater. Sci. Eng. A 400–401 (2005) 409–412.
[21] F. Appel, T. K. Heckel, H.-J. Christ, Electron microscope characterization of low cycle fatigue in a high-strength multiphase titanium aluminide alloy, Int. J. Fatigue 32 (2010) 792–798.
[22] F. Appel, D. Herrmann, F.D. Fischer, J. Svoboda, E. Kozeschnik, Role of vacancies in work hardening and fatigue of TiAl alloys, Int. J. Plasticity (2012), doi: http://dx.doi.org/10.1016/j.ijplas.2012.10.001
[23] M. Roth, H. Biermann, Thermomechanical fatigue behavior of the intermetallic γ-TiAl alloy TNB-V5 with different microstructures. Metall. Mater. Trans. A 41 (2010) 717-726.
[24] M. Roth, H. Biermann, Thermo-mechanical fatigue behaviour of a modern c-TiAl alloy, Int. Jour. Fatigue 30 (2008) 352–356.
[25] M. Roth, PhD Thesis, Behaviour and fatigue life of a intermetallic alloy on the basis of g-TiAl under thermo-mechanical loading, TU Bergakademie Freiberg (2010) 34-60.
[26] Crystallographica, Free software, Oxford Cryosystems Ltd, 3 Blenheim Office Park, Long Hanborough, Oxford OX29 8LN, United Kingdom

Figure captions

Figure 1: Duplex microstructure of the investigated γ-TiAl - alloy TNB-V5 consisting globular γ-TiAl grains and colonies of α_2/γ-TiAl lamellae. SEM micrograph using backscattered electron contrast

Figure 2: Cyclic deformation curve (a) and stress-strain hysteresis loops (b) of an in-phase thermo-mechanical fatigue test of a DP - TNB-V5 alloy with $\varepsilon_{a,mech} = 5.75 \times 10^{-3}$ in the temperature interval 673 K ≤ T ≤ 923 K [25].

Figure 3: Inverted ECCI images (a,d) and results of EBSD measurements (b,c,e,f) on a TiAl specimen after in-phase thermo-mechanical fatigue test with $\varepsilon_{a,mech} = 5.75 \times 10^{-3}$ in the temperature interval 673 K ≤ T ≤ 923 K up to failure at $N_f = 742$ cycles. (b, e) grain orientation maps coloured according to colour code of the stereographic standard triangle of the surface normal direction. (c, f) EBSD phase maps – green colour: γ-TiAl (P4/mmm), red colour: α_2-TiAl (P63/mmc), black: zero solutions). (a, b, c) Area of interest I. (d, e, f) Area of interest II. Stress axis lies horizontal.

Figure 4: Inverted ECCI images of four individual grains out of area I shown Figure 3a. (a) Grain 1 – lamellar region γ-TiAl/α_2-TiAl. (b) Grain 2 – globular γ-TiAl. (c) Grain 3 – lamellar region γ-TiAl/α_2-TiAl. (d) Grain 4 – globular γ-TiAl. Stress axis lies horizontal.

Figure 5: Inverted ECCI images of four individual grains out of area II shown Figure 3d. (a) Grain 1 – globular γ-TiAl. (b) Grain 2 – globular γ-TiAl. (c) Grain 3 – lamellar region γ-TiAl/α_2-TiAl. (d) Grain 4 – globular γ-TiAl. Stress axis lies horizontal.

Figure 6: Dislocation arrangements in globular (a, b) and lamellar (c) γ-TiAl taken by bright-field transmission electron (BF-TE) detector in a SEM on a TEM foil. Acceleration voltage 30 kV, working distance 3 mm, probe current 100 pA, spot size 2 nm.

Figure 7: Inverted ECCI micrographs of a globular (a) and a lamellar (b) γ-TiAl phase in the electron opaque area of a TEM foil taken by backscattered electron detector in a HR-FE-SEM (MIRA3) under untilted conditions. Acceleration voltage 20 kV, working distance 8 mm, beam current 500 pA.

Figure 8: Inverted ECCI micrographs of globular (a,b) and lamellar (c,d) γ-TiAl phase in a bulk specimen area taken with a backscattered electron detector in SEM under untilted conditions. Acceleration voltage 20 kV, (a,b): working distance 8 mm, beam current 500 pA (MIRA3); (c,d) working distance 5 mm, 120 µm aperture, high-current mode (LEO 1530).

Figure 9: TEM micrographs of the dislocation arrangement in a globular γ-TiAl grain. (a) Overview of the globular grain with deformation micro twins running through the whole grain. The corresponding diffraction pattern of the grain is shown in the upper left corner. (b) Detailed view of Fig. 8a (marked white rectangle) showing long dislocation segments parallel to the [110] direction.

Figure 10: TEM micrographs of the dislocation arrangement in a globular γ-TiAl grain. (a) Stacking fault ribbon originating from one deformation twin; the γ-grain is oriented nearly parallel to [1-10] and a [002] two beam condition was used. (b) γ-lamellae oriented with [01-1] nearly parallel to the foil normal observed using a [111] two beam condition; the most obvious feature of the deformation structure are straight dislocation segments extending between the two lamellar boundaries.

Table captions

Table 1: Lattice parameters of the γ-TiAl phase and the α_2Ti_3Al-phase used for the EBSD-measurements [26]

Table 2: Crystallographic orientation given in Euler angles, g-matrix and (hkl)[uvw] for the grains labeled in Figure 3a and 3d. .

Scanning and transmission electron microscopy investigations of defect arrangements in a two-phase γ-TiAl alloy

A. Weidner[a*)], F. Pyczak[b)], H. Biermann[a)]

[a)] Institute of Materials Engineering, Technische Universität Bergakademie Freiberg, Gustav-Zeuner-Str. 5, 09596 Freiberg, Germany

[b)] Institute of Materials Research, Department of Metal Physics, Helmholtz-Zentrum Geesthacht, Max-Planck-Str. 1, 21502 Geesthacht, Germany

Abstract

Different methods of scanning and transmission electron microscopy (SEM, TEM) were applied on a γ-TiAl alloy TNB-V5 after a thermo-mechanical fatigue test. Electron channelling contrast imaging (ECCI) and electron backscattered diffraction were carried out on bulk specimen. In addition, ECCI and scanning transmission electron microscopy in the SEM were carried out on a TEM-foil in the electron opaque and the electron transparent region, respectively. The investigations were completed by transmission electron microscopy in form of standard bright field imaging as well as by taking corresponding diffraction patterns. The results demonstrate in an impressive way that the ECCI technique applied in scanning electron microscope can successfully supplement or in some cases replace imaging of dislocation arrangements in TEM.

Keywords

Titanium aluminide alloys, electron channelling contrast imaging, transmission electron microscopy, EBSD

1. Introduction

The commonly used technique for the investigation of the deformation microstructure on the nano/micro scale is transmission electron microscopy (TEM). It allows the investigation of lattice defects like dislocations, stacking faults and/or micro twins in individual grains. In addition, information on the crystallographic orientation of the investigated grain is available. However, the investigated number of grains is very restricted due to the limited size of the electron transparent region. In this context, advanced techniques applied in scanning electron microscope help to overcome these restrictions. Complementary to TEM, the combination of electron channelling contrast imaging (ECCI) technique and electron backscattered diffraction (EBSD) in a high-resolution field emission SEM (HR-FE-SEM) can be applied to bulk specimens.

The ECCI technique can be used for the characterization of microstructures after plastic deformation, e.g. [1-5], because it allows the visualization of condensed dislocation arrangements near the surface of bulk specimens, e.g. dislocation walls/cells after fatigue [1, 6-9]. Even the imaging of individual dislocations [5, 10-12] is possible under defined diffraction conditions. The main advantages of the ECCI technique compared to transmission electron microscopy (TEM) are that (i) images can be taken from bulk specimens making this technique very attractive for the examination of defects during in-situ deformation and (ii) much better statistics on the dislocation arrangements can be obtained. The application of

[*] Corresponding author: Tel.: +49-3731-39 2124, Fax: +49-3731-39 3703,
email-address: weidner@ww.tu-freiberg.de

the ECCI technique in combination with EBSD measurements in a SEM gives a great potential for investigating and improving the knowledge on the underlying deformation mechanisms and to clarify the deformation behaviour of metals, e.g. tensile and cyclic deformation of TRIP steels [11-12]. ECCI performed under exact Bragg condition reveals excellent contrast for investigations of dislocations [13]. Defects like individual dislocations lead to a local lattice distortion and as a consequence the Bragg condition is locally not fulfilled. Therefore, individual dislocations will appear as bright lines in a dark matrix. Applying an inverted signal of BSE contrast, inverted ECC images are obtained, where dislocations appear as dark lines in a bright matrix in analogy to TEM bright field micrographs.

Titanium aluminide (γ-TiAl) alloys with their low density (3.7 – 4.7 g/cm³), high melting temperature (in the range of 1700 K) and good oxidation resistance are attractive candidates for high temperature applications in the automotive and aerospace industry and have been in focus of scientific interest since many years [14]. Most γ-TiAl alloys are based on a two phase microstructure which contains the tetragonal γ-TiAl phase with a $L1_0$-structure and the hexagonal α_2-Ti_3Al phase with a DO_{19}-structure. Four different types of microstructures formed by these two phases are known [15]: near gamma (NG), duplex (DP), nearly lamellar (NL) and fully lamellar (FL). γ - TiAl alloys of the 3rd generation containing higher concentrations of Nb (5 - 10 %) exhibit a high strength combined with acceptable room temperature ductility and damage tolerance due to their fine-grained microstructure.

The deformation behaviour of the γ-phase is determined by dislocation glide processes in the $L1_0$-structure [16]. Dislocation glide is activated on {111} γ planes along the close packed directions <110>. Both, ordinary dislocations of Burgers vector b = ½ <110] as well as super dislocations with the Burgers vector b = ½ <112] or b = <101] can occur. A second possible deformation mechanism is the formation of deformation twins along 1/6 <11-2] on the {111} γ plane. The complex dissociation in partial dislocations forming planar defects like antiphase boundaries or stacking faults was observed for super dislocations of type ½ <112] and <101] [17]. A dissociation in partial dislocations is not reported for ordinary dislocations of type ½ <110]. The deformation behaviour of two phase γ-TiAl alloys up to high temperatures (973 K) is determined by the easy activation of <110] dislocation glide and mechanical twinning [17]. The motion of super dislocations is suppressed in that temperature regime [18]. Henaff et al. [19] showed that in Ti-48Al-2Nb-2Cr specimens which experienced LCF at temperatures as low as 723 K the dislocation structure consists of ordinary dislocations which showed signs of recovery and climb processes. Corresponding features are also remnant dislocation loops, which were reported by Jouiad et al. [20] in the same alloy for LCF at 1023 K. Also Appel et al. [21] found climbed and cross slipped dislocation segments in a Ti-45Al-8Nb-0.2C alloy after LCF at 823 K. But, besides these features also dense dislocation walls are reported by Appel et al. [22] in the same alloy also at 823 K.

The main objective of the present paper is to demonstrate the application of the ECCI technique to study the dislocation arrangements in comparison with TEM investigations and STEM investigations in a SEM. For these investigations the γ-TiAl alloy (TNB-V5) with a duplex microstructure after a thermo-mechanical fatigue test [23] was chosen.

2. Material and deformation tests

Investigations of the microstructure after a thermo-mechanical fatigue test were carried out on the γ-TiAl alloy TNB-V5. The material with the nominal chemical composition Ti-45Al-5Nb-0.2C-0.2B (at %) was produced by Plansee AG (Reutte). The investigated material showed a so-called duplex structure with 40 % of globular γ-TiAl grains and 60 % of lamellar colonies with γ/α_2-lamellae. The mean grain size of globular γ-TiAl grains is about 2 to 4 µm, the size of lamellar colonies ranges from 5 to 25 µm and the inter lamellar spacing varies from 50 to 500 nm. Figure 1 shows an overview of the duplex microstructure (SEM micrograph, backscattered electron contrast).

Insert Figure 1 about here

The TMF test was performed on a compact cylindrical specimen with a gauge length of 19 mm and a gauge diameter of 7.0 mm. The specimen surface was electrolytically polished. The TMF test was carried out on a servo hydraulic testing system under total-strain control mode with a mechanical strain amplitude of $\varepsilon_{a,mech} = 5.75 \times 10^{-3}$ and a strain rate of 9.20×10^{-5} s^{-1} [23]. The applied temperature interval was 673 K ≤ T ≤ 923 K. The TMF temperature–strain cycles were applied in-phase (IP) and both, the mechanical strain cycles and the temperature cycles had a triangular shape. The specimen was heated with a high frequency induction heater and a heating rate of 2 K/s. Axial temperature deviations within the gauge length were below ±5 K [24]. The corresponding cyclic deformation curve and stress-strain hysteresis loops are shown in Figure 2. Initially, the stress amplitude slightly decreases reaching saturation at about 10 numbers of cycles. Furthermore, it becomes evident from the stress-strain hysteresis loops that a compressive mean stress is present from the beginning of deformation. This compressive mean stress is increasing with ongoing deformation as a result of a decreasing upper stress [25].

Insert Figure 2 about here

After failure at $N_f = 742$ cycles, the specimen was cut parallel to the loading axis. One half of the specimen was prepared for SEM investigations. From the other part TEM foils were prepared. EBSD and ECCI investigations on the bulk specimens were performed in the plane parallel to the loading axis using field emission scanning electron microscopes (LEO 1530 from ZEISS, MIRA3 XMU from TESCAN). The OIM software from TSL was used for EBSD measurements under a specimen tilt of 70° and an acceleration voltage of 20 kV. The ECCI investigations were performed using a retractable four-quadrant backscattered electron detector allowing working distances of 8 mm. The MIRA 3 XMU is working with a single aperture of 10 µm. The beam current can be adjusted continuously up to 100 nA. Information about the effective probe current and the resulting spot diameter on the specimen surface are always available due to the real time “in-flight beam tracing” technology. ECCI investigations were performed at an acceleration voltage of 20 kV using a 10 µm aperture and a probe current < 2 nA. The lattice parameters, which were used for the phase identification by EBSD, are summarized in Tab. 1.

Insert Table 1 about here

Normally, the best surface state of specimens for ECCI investigations is obtained by electrolytic polishing. However, in multiphase materials like the present TiAl-TNB-V5 alloy electrolytic polishing leads to a pronounced surface relief. A method to avoid such a pronounced surface relief is vibration polishing (Buehler) for about 24 hours. The removal of material is very gentle. Therefore, by this method a very smooth and deformation free surface is obtained.

The specimens for TEM investigations were prepared perpendicular to the external load axis. A cylinder with a diameter of 3 mm was machined by spark erosion. Discs with a thickness of approximately 300 µm were cut and ground up to a final thickness of 150 µm. The discs were electrolytically thinned to electron transparency using a mixture of methanol (60%), butanol (34%) and perchloric acid (6%) as agent at a temperature of 243 K and a voltage of 25 V. The TEM investigations were performed in a Philips CM200 with an acceleration voltage of 200 kV.

Additionally, the TEM foils were investigated in the FE-SEM (MIRA3) applying ECCI as well as using a transmission electron (TE) detector. The TE detector can be used in bright-field and dark-field mode. The TE detector was mounted directly on the SEM specimen stage. The working distance is 3 mm. Best imaging conditions were obtained at an acceleration voltage of 30 kV and a beam current of 100 pA.

3. Results and discussion

3.1 SEM investigation – EBSD and ECCI

Figure 3 shows two examples of SEM investigations on the TiAl specimen. Inverted ECCI images (a,d) are shown together with EBSD grain orientation maps (b,e) and EBSD phase maps (c,f) of two areas of interest. The grain orientation maps are coloured according to the colour code of the stereographic standard triangle of the surface normal direction. In the phase maps the green colour represents γ-TiAl and the red colour α_2-Ti_3Al. In the lamellar regions alternating lamellae of γ-TiAl and α_2-Ti_3Al were detected if the α_2-Ti_3Al lamellae are thick enough. Two different areas of interest were chosen in order to demonstrate the great variance of microstructural features, which becomes evident from the ECCI overview images. Even without additional tilting/rotating of the specimen, several individual grains are in perfect imaging conditions for visualization of microstructural details like twins or dislocations. Already from the overview ECCI images of the whole areas of interest it is possible to distinguish several different “internal” structures inside individual γ-TiAl grains or in the lamellar regions. Four individual grains were labelled in Figures 3a and d, respectively. For these grains inverted ECCI images were taken at higher magnification in order to illustrate the microstructural features developed during thermo-mechanical fatigue. These high-resolution ECCI images are summarized in Figure 5 for area I and in Figure 6 for area II. The crystallographic orientations of these individual grains are summarized in Table 2.

The inverted ECCI micrographs in Figure 4 show the internal structure both in γ-TiAl lamellae in the lamellar regions (a, c) as well as in the globular γ-TiAl grains. In all cases the specimen was not tilted and the grain orientation was used as it is for the ECCI investigations. The crystallographic orientation of these grains can be obtained from the EBSD grain orientation map in Fig. 3b and 3e and Table 2, respectively. In the lamellar regions the dark areas correspond to the hexagonal α_2-Ti_3Al phase. In all four grains individual dislocations can be

clearly detected. Figure 4b shows in addition mechanically formed micro twins (marked by arrows).

Insert Figure 3 about here

Insert Figure 4 about here

In addition, between these micro twins individual dislocations are visible running along different directions. In Figure 4c a slightly disoriented subgrain structure becomes visible. Figure 4d represents an example for elongated individual dislocations, which seem to be pinned. Based on alloy composition the black particles which frequently pin dislocations (indicated by arrows) could either be borides or carbides. No attempt to identify them e.g. by diffraction in TEM was undertaken, while they are too small for EBSD/EDX analysis in SEM.

Figure 5 shows additional microstructural features. Figure 5a contains at least 4 different features: (i) long individual dislocations, (ii) dislocation tangles, (iii) micro twins and (iv) stacking fault contrast originated by a micro twin (marked by arrows). In Figure 5b two small γ-TiAl grains with nearly the same surface normal direction are shown. However, the left grain contains dislocation tangles, whereas in the right grain micro twins (arrows) and elongated individual dislocations between these micro twins are visible. The formation of micro twins is well illustrated in Figure 5c (arrows). Moreover, the formation of a subgrain structure containing several individual dislocations is visible, too. Figure 5d illustrates again a dislocation arrangement consisting of elongated dislocations, which are pinned at their ends (arrows) as well as of dislocation tangles.

Insert Figure 5 about here

3.2 SEM investigation on a TEM-foil

A TEM foil from the same deformation state was studied in an HR-FE-SEM. Both, the electron transparent region as well as the electron opaque area were investigated by application of two different techniques. First, the bright-field transmission electron detector was used. Figure 6 shows dislocation arrangements in globular (a, b) and lamellar (c) γ-TiAl areas.

Figure 6a is comparable to Fig. 4b and Fig. 5a-c. It shows narrow bands running through the whole grain which are most probably twins. Also long dislocation segments inclined to the micro twins are visible. Some of the segments are pinned by obstacles resulting in the bow-out structure. Also debris and small dipole loops become visible. Even in very thin γ-TiAl areas between α_2-Ti_3Al lamellae dislocation arrangements can be imaged. Unfortunately, it is impossible to obtain directly information on the crystallographic orientation of the investigated grains. For this purpose, the detour via EBSD measurements on the TEM foil is necessary. Moreover, detailed burgers vector analysis seems to be difficult by this technique because the possibility for tilting the specimen is very limited due to the low working distance of 3 mm. The area for investigations is limited to electron transparent regions like for TEM investigations. However, it should be noted that TE images in the SEM were obtained at an acceleration voltage of 30 kV in contrast to the acceleration voltages between 80 and 300 kV conventional TEMs are working at.

Insert Figure 6 about here

The rather limited statistics of grains accessible for investigation in the electron transparent area of a TEM foil can be improved significantly by applying the ECCI technique to the electron opaque areas of TEM foils or on bulk specimens. Figures 7 and 8 show dislocation arrangements in globular γ-TiAl grains of a TEM foil and a bulk specimen, respectively. Micro twins, long screw dislocation segments, dislocation segments pinned by obstacles, debris and dislocation loops are visible in ECCI contrast. Even in the narrow γ-phase lamellae with a typical thickness < 500 nm individual dislocations and micro twins are detectable (Fig. 8d). γ-phase lamellae show a fragmentation either by micro twins or by specific dislocation arrangements. The main advantage applying ECCI on bulk specimens, i.e. high grain statistic, becomes evident from the following fact. Although all micrographs were taken on the specimen just as mounted on the SEM stage without knowing the individual crystallographic orientation, a large number of grains are in good diffraction conditions for imaging dislocation arrangements without additional tilting and rotating the specimen. Therefore, ECCI on bulk specimens is a good way to obtain a statistically sound overview of the deformation microstructure, especially dislocations and twins. Nevertheless, for an exact description of the crystallographic nature of dislocation arrangements information about the exact diffraction conditions is necessary. Performing EBSD measurements before or after the ECCI investigation on the same area can provide the crystallographic orientation of each individual investigated grain. By this, the exact diffraction conditions can be calculated for certain types of dislocations.

Insert Figure 7 about here

Insert Figure 8 about here

3.3 TEM investigations

In order to verify the information of the SEM studies and to get more detailed information on the type of dislocations activated during the thermo-mechanical fatigue test and other microstructural features additional TEM investigations were performed. In a γ-grain oriented close to the [1-10] zone axis micrographs were recorded under two beam conditions using the (111), (220), (11-1) and (002) reflections. Figure 8 shows an overview of the γ-grain under investigation with the indexed diffraction pattern of the γ-phase as an inset. The micrograph in Figure 9a was recorded using a (111) reflection two beam condition and shows a number of deformation twins stretching over the whole grain while long dislocation segments are found which lie inclined to these twins. All dislocations are out of contrast when using a [002] two beam condition. This is an indication that no super dislocations are present in this grain. Figure 9b shows a part of this γ-grain in higher magnification using the same imaging conditions. By comparing the trace of the (11-1) plane which is marked by a dashed line with the direction of the twins it is obvious that the deformation twins lie in this crystallographic plane. They do not appear as lines because the foil was slightly tilted away from the [1-10] zone axis for recording Figure 9b under the [111] two beam condition. The dislocation segments are mainly oriented parallel to the [110] direction which is indicated by an arrow. No complete Burgers vector analysis was performed, but as the majority of dislocations are out of contrast using the [002] diffraction vector and show contrast using the [110] diffraction vector they are probably ordinary dislocations of the Burgers vector $b = \pm \frac{1}{2}$ [110] type. Accordingly, the majority of dislocation segments are parallel to [110] and hence

of screw character. Some dislocation segments are bowed out. The observed micro twins and the dislocation arrangement between these micro twins are comparable to those imaged applying the ECCI technique on a bulk specimen as shown in Figure 4d.

Insert Figure 9 about here

From Figure 9b it is clear that these bowed-out sections of dislocations are pinned by small obstacles. In addition, in Figure 8b also other features like debris and remnant dislocation loops are visible. These features are normally associated in literature [16] with excess vacancies which act as dislocation obstacles, remnant dislocation dipoles developing at jogs and by-products of dislocation climb and multiplication processes. As the present study concentrates on comparison of different microscopy methods and not on deformation structures in TiAl-alloys the reader is kindly referred to the literature for more details. Nevertheless, it is noteworthy that similar features are reported for TiAl specimens after LCF in the 723 – 823 K regime [19-21].

Another feature of the deformation structure is revealed in Figure 10a. Here, a stacking fault is observed using the (002) reflection. This stacking fault starts at the boundary of a deformation twin and is probably associated with slip transfer through this twin boundary. It is not a single stacking fault but a stacking fault ribbon generated by the successive glide of a number of partial dislocations. Also in the lamellar region of the microstructure deformation in the γ-phase is mainly associated with dislocation movement. Figure 10b shows long dislocation segments in a lamellar γ-TiAl microstructure running between Ti_3Al lamellae. Overall the features pictured by TEM in this specimen correspond very well with the micrographs obtained by ECCI and STEM in the SEM in the same TMF specimen.

Insert Figure 10 about here

4. Summary

The present investigations showed a comparison between different advanced techniques of scanning electron microscopy and transmission electron microscopy.

Investigations on the microstructure of the γ-TiAl alloy TNB-V5 after thermo-mechanical fatigue tests were performed by scanning and transmission electron microscopy. The main goal of the presented results was to demonstrate that the application of the ECCI technique on bulk specimens as well as on TEM-foils is a very powerful method to study the arrangements of deformation induced defects like micro twins, stacking faults and/or regular dislocations. The shown microstructural features are already well known from the literature and are the same as in the isothermal LCF regime.

The results obtained from combined EBSD and ECCI investigations on the bulk specimen demonstrate vividly that dislocation structures can be visualized both in the globular γ-TiAl grains as well as in the γ-TiAl lamellae of the lamellar regions (alternating γ-TiAl and α_2-Ti_3Al lamellae). The visualized defect types and/or arrangements by application of ECCI technique are in resolution comparable to those obtained from STEM or TEM investigations. It becomes evident from the presented ECCI investigations that on a bulk specimen the investigation of dislocation and/or defect arrangements can be performed with a reasonable good statistics. In combination with EBSD it is even possible to investigate the influence of crystallographic orientation with a reasonable time exposure.

Acknowledgment

Dr. M. Roth is gratefully acknowledged for the providing the TiAl specimens after thermo-mechanical fatigue. The authors thank Ms. A. Müller and Ms. K. Zuber from the Institute of Materials Science for careful preparation of TiAl specimens for EBSD and ECCI investigations.

References

[1] R. Zauter, F. Petry, M. Bayerlein, C. Sommer, H.-J. Christ, H. Mughrabi, Electron channelling contrast as a supplementary method for microstructural investigations in deformed metals, Phil. Mag. A 66 (1992) 425-436.

[2] A. J. Wilkinson, G. R. Anstis, J. T. Czernuszka, N.J. Long, P. B. Hirsch, Electron channelling contrast imaging of interfacial defects in strained silicon- germanium layers on silicon, Phil. Mag. A 68 (1993) 59-80.

[3] A. J. Wilkinson, P. B. Hirsch, Electron Diffraction Based Techniques in Scanning Electron Microscopy of Bulk Materials, Micron 28 (1997) 279-308.

[4] B. C. Ng, B. A. Simkin, M. A. Crimp, Application of the electron channeling contrast imaging technique to the study of dislocations associated with cracks in bulk specimens, Ultramicroscopy 75 (1998) 137145.

[5] I. Gutierrez-Urrutia, S. Zaefferer, D. Raabe, Electron channeling contrast imaging of twins and dislocations in twinning-induced plasticity steels under controlled diffraction conditions in a scanning electron microscope, Scripta Mater. 61 (2009) 737-740.

[6] B. A. Simkin, B. C. Ng, M. A. Crimp, Microscopy and Analysis (1999) 11.

[7] C. Buque, J. Bretschneider, A. Schwab, C. Holste, Mater. Sci. Eng. A 300 (2001) 254.

[8] Z. F. Zhang, Z. G. Wang, Z. M. Sun, Evolution and microstructural characterization of deformation bands in fatigued copper single crystals, Acta Mater. 49 (2001) 2875-2886.

[9] Y. Kaneko, K. Fukui, S. Hashimoto, Electron channeling contrast imaging of dislocation structures in fatigued austenitic stainless steels Mater. Sci. Eng. A 400-401 (2005) 413.

[10] A. Weidner, J. Man, W. Skrotzki, J. Polák, Slip Localization and Dislocation Structure at Early Stages of Fatigue Damage in Austenitic Stainless Steel (316L)Proceedings ICF12, Ottawa, (2009) CD-ROM fin00681.

[11] A. Weidner, S. Martin, V. Klemm, U. Martin, H. Biermann, Stacking faults in high-alloyed metastable austenitic cast steel observed by electron channelling contrast imaging, Scripta Mater. 64 (2011) 513–516.

[12] A. Weidner, A. Glage, L. Sperling, H. Biermann, Observation of stacking faults in a scanning electron microscope by electron channelling contrast imaging, Int. J. Mat. Res. (formerly Z. Metallkd.) 102 (2011)1-3.

[13] I. Gutierrez-Urrutia, D. Raabe, Dislocation density measurement by electron channelling contrast imaging in a scanning electron microscope, Scripta Mater. 66 (2012) 343-346.

[14] G.H. Meier, N. Birks, F.S.Pettit, R.A. Perkins, H.J. Grabke, Environmental behaviour of intermetallic materials, in: Strucutral Intermetallics, R. Darolia, j.J. Lewandowski, C.T. Liu, P.L. Martin, D.B. Miracle, M.V. Nathal (editors), TMS, Warrendale (1993) 861.

[15] Y.-W. Kim, D.M. Dimiduk, Progress in the understanding of gamma titanium aluminides. JOM 43 (1991) 40.

[16] F. Appel, R. Wagner, Microstructure and deformation of two-phase γ- titanium aluminides, Materials Science and Engineering R 22 (1998) 187-268.

[17] B.J. Inkson, C.J. Humphreys, High resolution electron microscopy observation of ½ <112> superdislocation in TiAl, Phil. Mag. Letters 71 (1995) 307.
[18] V.K. Vasudevan, M.A. Stucke, S.A. Court, H.L. Fraser, The influence of second phase Ti3Al on the deformation mechanisms in TiAl, Phil. Mag. Letters 59 (1989) 299.
[19] G. Henaff, A.-L. Gloanec, Fatigue properties of TiAl alloys, Intermetallics 13 (2005) 543–558.
[20] M. Jouiad, A.-L. Gloanec, M. Grange, G. Henaff, Cyclic deformation mechanisms in a cast gamma titanium aluminide alloy, Mater. Sci. Eng. A 400–401 (2005) 409–412.
[21] F. Appel, T. K. Heckel, H.-J. Christ, Electron microscope characterization of low cycle fatigue in a high-strength multiphase titanium aluminide alloy, Int. J. Fatigue 32 (2010) 792–798.
[22] F. Appel, D. Herrmann, F.D. Fischer, J. Svoboda, E. Kozeschnik, Role of vacancies in work hardening and fatigue of TiAl alloys, Int. J. Plasticity (2012), doi: http://dx.doi.org/10.1016/j.ijplas.2012.10.001
[23] M. Roth, H. Biermann, Thermomechanical fatigue behavior of the intermetallic γ-TiAl alloy TNB-V5 with different microstructures. Metall. Mater. Trans. A 41 (2010) 717-726.
[24] M. Roth, H. Biermann, Thermo-mechanical fatigue behaviour of a modern c-TiAl alloy, Int. Jour. Fatigue 30 (2008) 352–356.
[25] M. Roth, PhD Thesis, Behaviour and fatigue life of a intermetallic alloy on the basis of g-TiAl under thermo-mechanical loading, TU Bergakademie Freiberg (2010) 34-60.
[26] Crystallographica, Free software, Oxford Cryosystems Ltd, 3 Blenheim Office Park, Long Hanborough, Oxford OX29 8LN, United Kingdom

Figure captions

Figure 1: Duplex microstructure of the investigated γ-TiAl - alloy TNB-V5 consisting globular γ-TiAl grains and colonies of α_2/γ-TiAl lamellae. SEM micrograph using backscattered electron contrast

Figure 2: Cyclic deformation curve (a) and stress-strain hysteresis loops (b) of an in-phase thermo-mechanical fatigue test of a DP - TNB-V5 alloy with $\varepsilon_{a,mech} = 5.75 \times 10^{-3}$ in the temperature interval 673 K ≤ T ≤ 923 K [25].

Figure 3: Inverted ECCI images (a,d) and results of EBSD measurements (b,c,e,f) on a TiAl specimen after in-phase thermo-mechanical fatigue test with $\varepsilon_{a,mech} = 5.75 \times 10^{-3}$ in the temperature interval 673 K ≤ T ≤ 923 K up to failure at $N_f = 742$ cycles. (b, e) grain orientation maps coloured according to colour code of the stereographic standard triangle of the surface normal direction. (c, f) EBSD phase maps – green colour: γ-TiAl (P4/mmm), red colour: α_2-TiAl (P63/mmc), black: zero solutions). (a, b, c) Area of interest I. (d, e, f) Area of interest II. Stress axis lies horizontal.

Figure 4: Inverted ECCI images of four individual grains out of area I shown Figure 3a. (a) Grain 1 – lamellar region γ-TiAl/α_2-TiAl. (b) Grain 2 – globular γ-TiAl. (c) Grain 3 – lamellar region γ-TiAl/α_2-TiAl. (d) Grain 4 – globular γ-TiAl. Stress axis lies horizontal.

Figure 5: Inverted ECCI images of four individual grains out of area II shown Figure 3a. (a) Grain 1 – globular γ-TiAl. (b) Grain 2 – globular γ-TiAl. (c) Grain 3 – lamellar region γ-TiAl/α_2-TiAl. (d) Grain 4 – globular γ-TiAl. Stress axis lies horizontal.

Figure 6: Dislocation arrangements in globular (a, b) and lamellar (c) γ-TiAl taken by bright-field transmission electron (BF-TE) detector in a SEM on a TEM foil. Acceleration voltage 30 kV, working distance 3 mm, probe current 100 pA, spot size 2 nm.

Figure 7: Inverted ECCI micrographs of a globular (a) and a lamellar (b) γ-TiAl phase in the electron opaque area of a TEM foil taken by backscattered electron detector in a HR-FE-SEM (MIRA3) under untilted conditions. Acceleration voltage 20 kV, working distance 8 mm, beam current 500 pA.

Figure 8: Inverted ECCI micrographs of globular (a,b) and lamellar (c,d) γ-TiAl phase in a bulk specimen area taken with a backscattered electron detector in SEM under untilted conditions. Acceleration voltage 20 kV, (a,b): working distance 8 mm, beam current 500 pA (MIRA3); (c,d) working distance 5 mm, 120 µm aperture, high-current mode (LEO 1530).

Figure 9: TEM micrographs of the dislocation arrangement in a globular γ-TiAl grain. (a) Overview of the globular grain with deformation micro twins running through the whole grain. The corresponding diffraction pattern of the grain is shown in the upper left corner. (b) Detailed view of Fig. 8a (marked white rectangle) showing long dislocation segments parallel to the [110] direction.

Figure 10: TEM micrographs of the dislocation arrangement in a globular γ-TiAl grain. (a) Stacking fault ribbon originating from one deformation twin; the γ-grain is oriented nearly parallel to [1-10] and a [002] two beam condition was used. (b) γ-lamellae oriented with [01-1] nearly parallel to the foil normal observed using a [111] two beam condition; the most obvious feature of the deformation structure are straight dislocation segments extending between the two lamellar boundaries.

Table captions

Table 1: Lattice parameters of the γ-TiAl phase and the α_2Ti_3Al-phase used for the EBSD-measurements [26]

Table 2: Crystallographic orientation given in Euler angles, g-matrix and (hkl)[uvw] for the grains labeled in Figure 3a and 3d. .

Figure_1.tif
Click here to download high resolution image

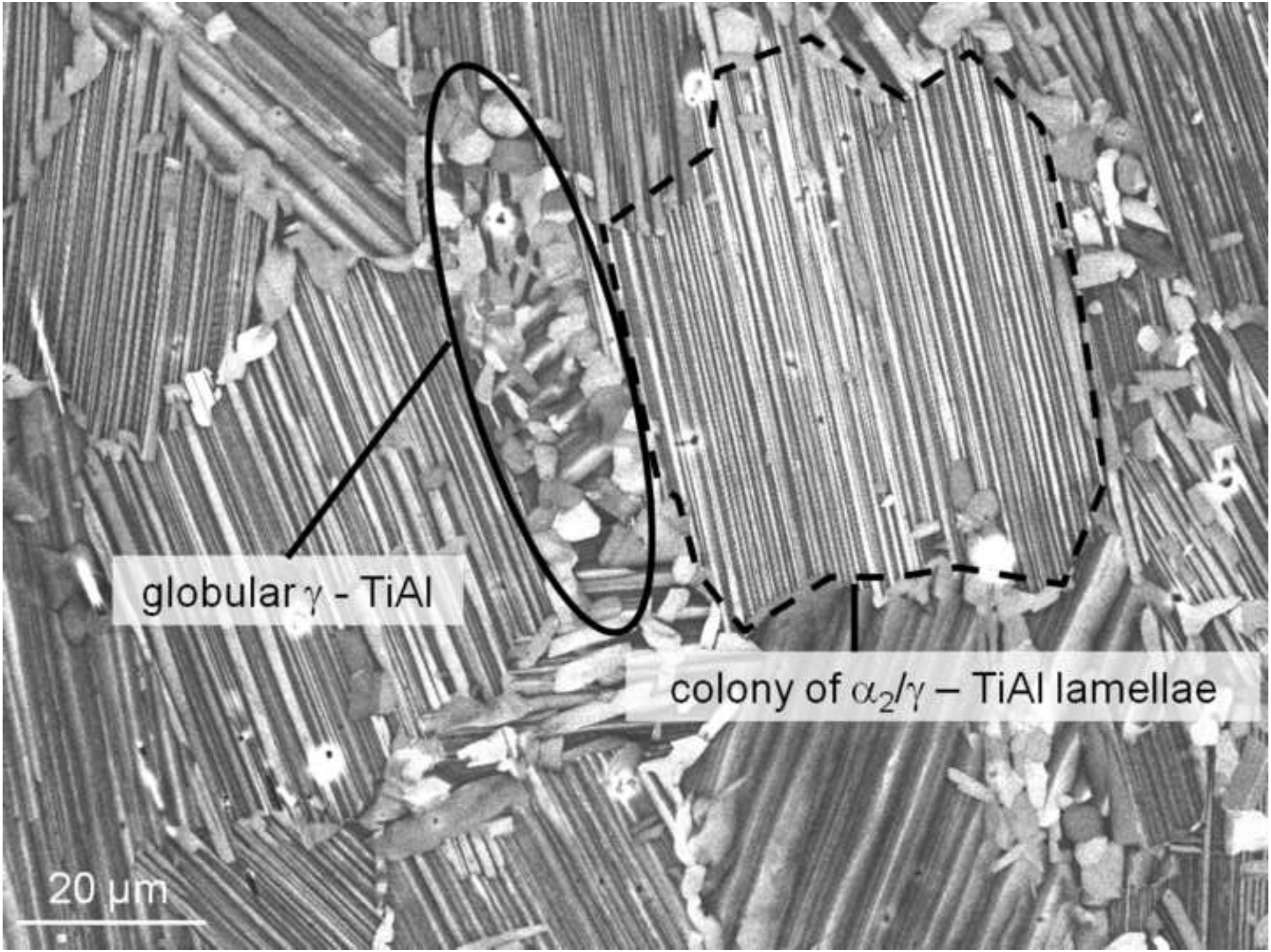

Figure_2a.tif
Click here to download high resolution image

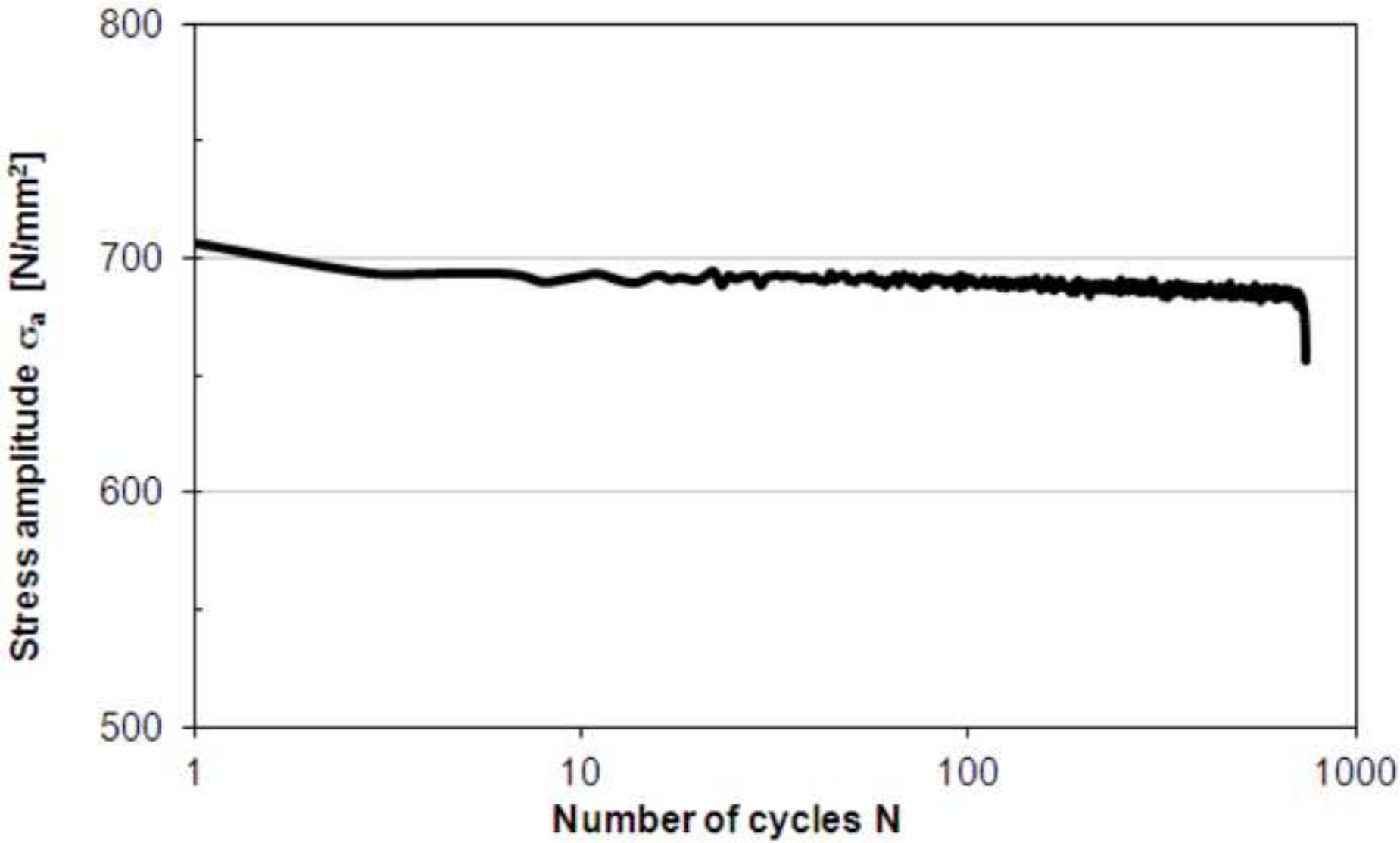

Figure_2b.tif
Click here to download high resolution image

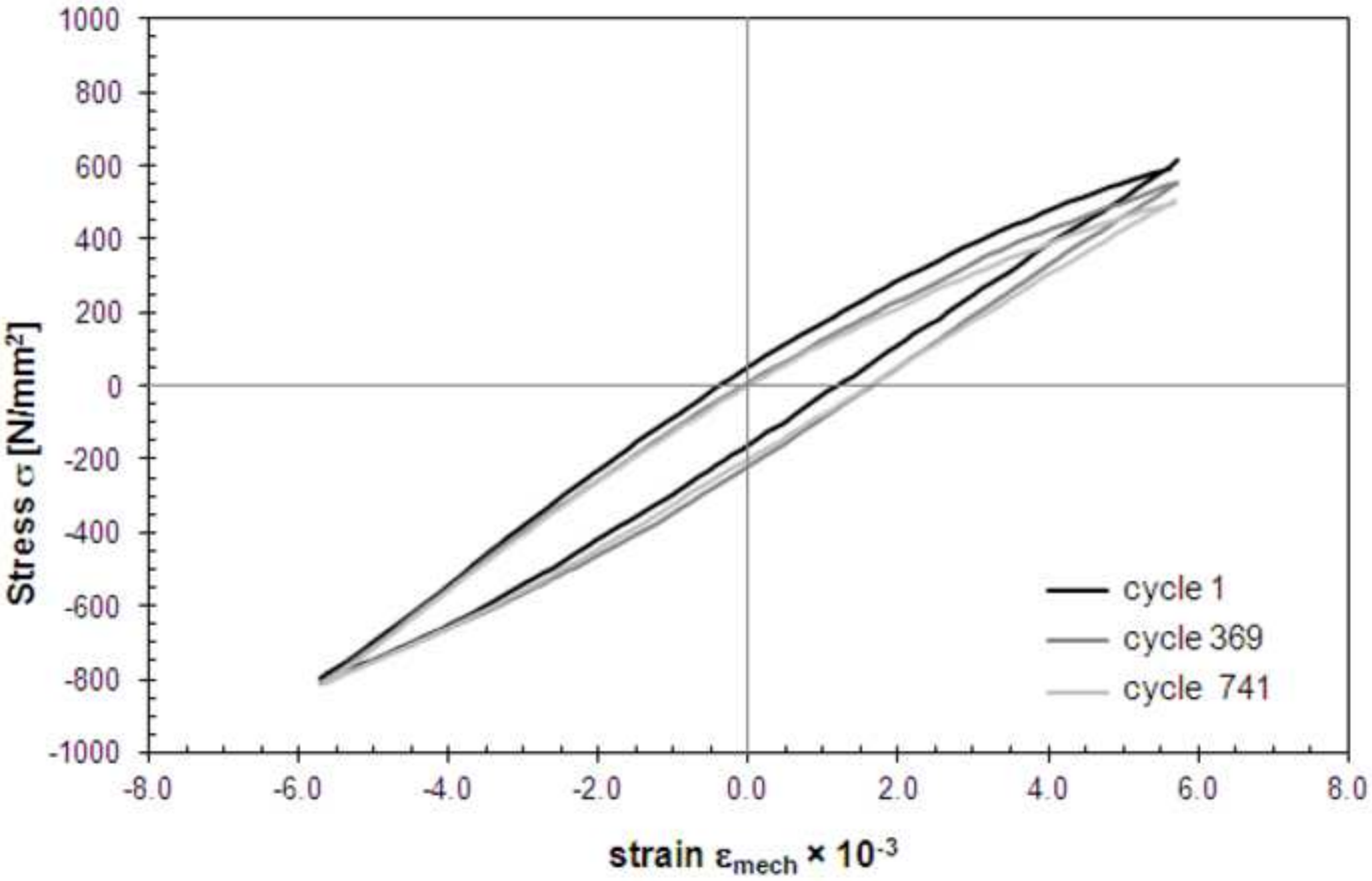

Figure_3.tif
Click here to download high resolution image

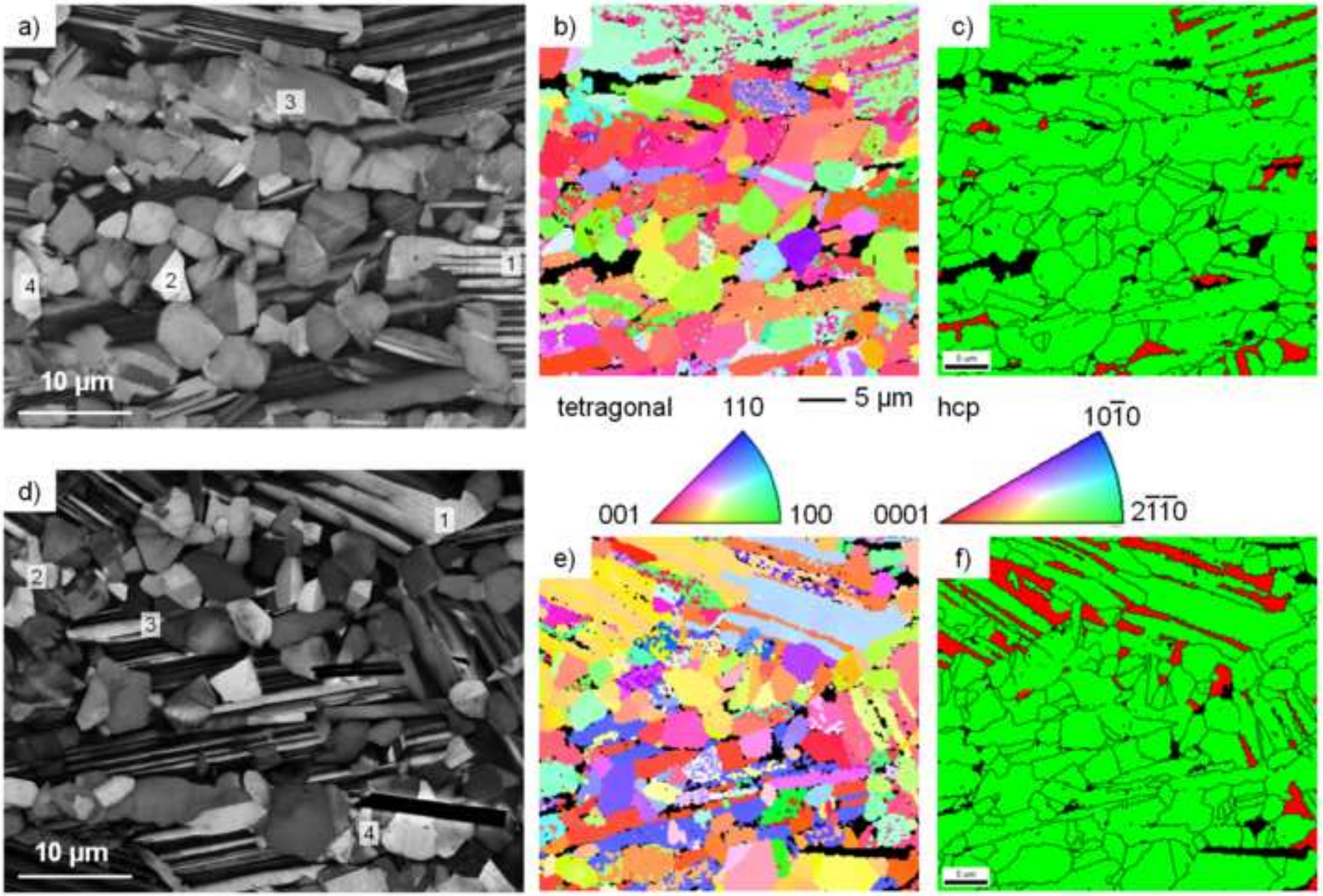

Figure_4.tif
Click here to download high resolution image

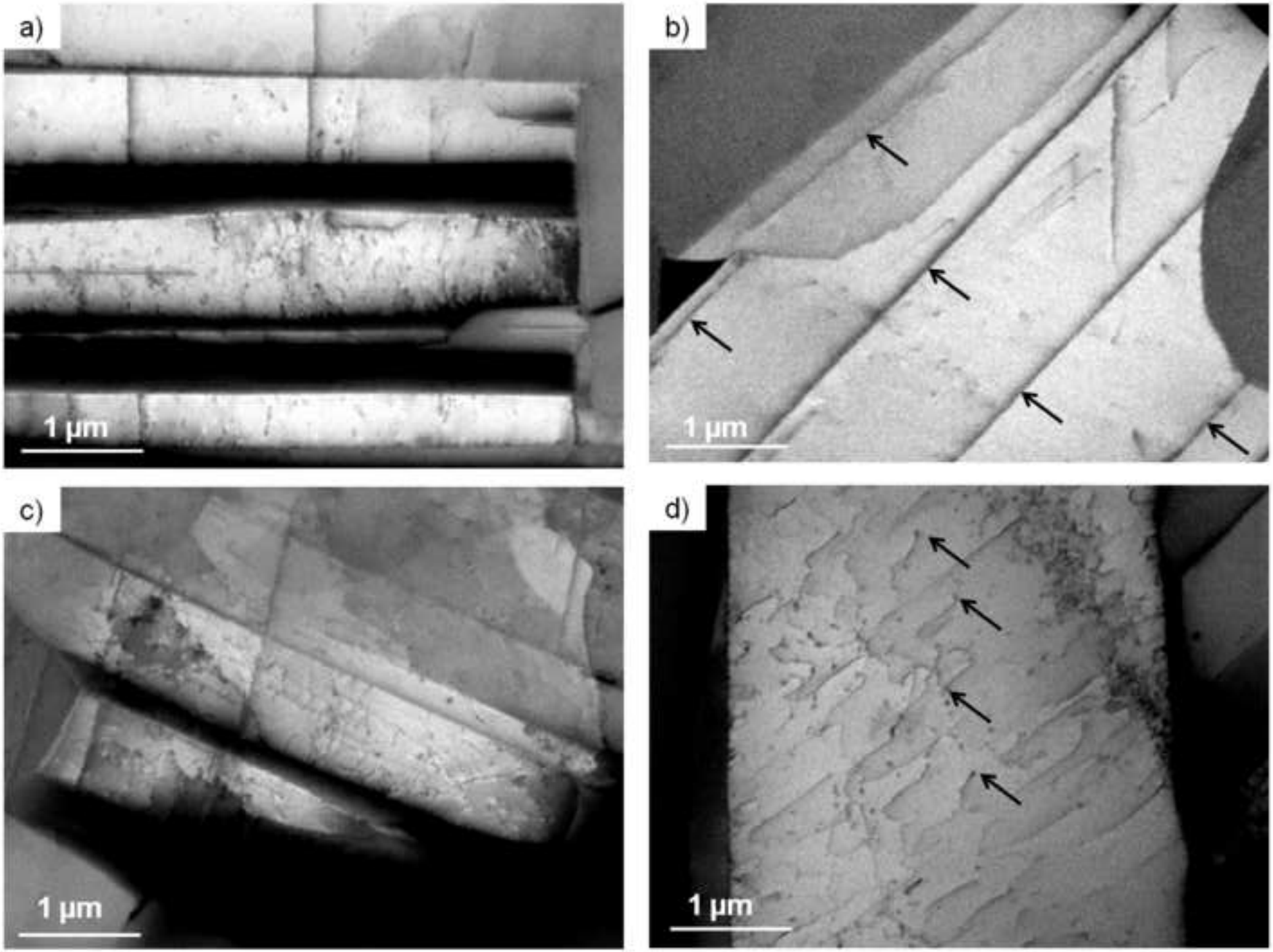

Figure_5.tif
Click here to download high resolution image

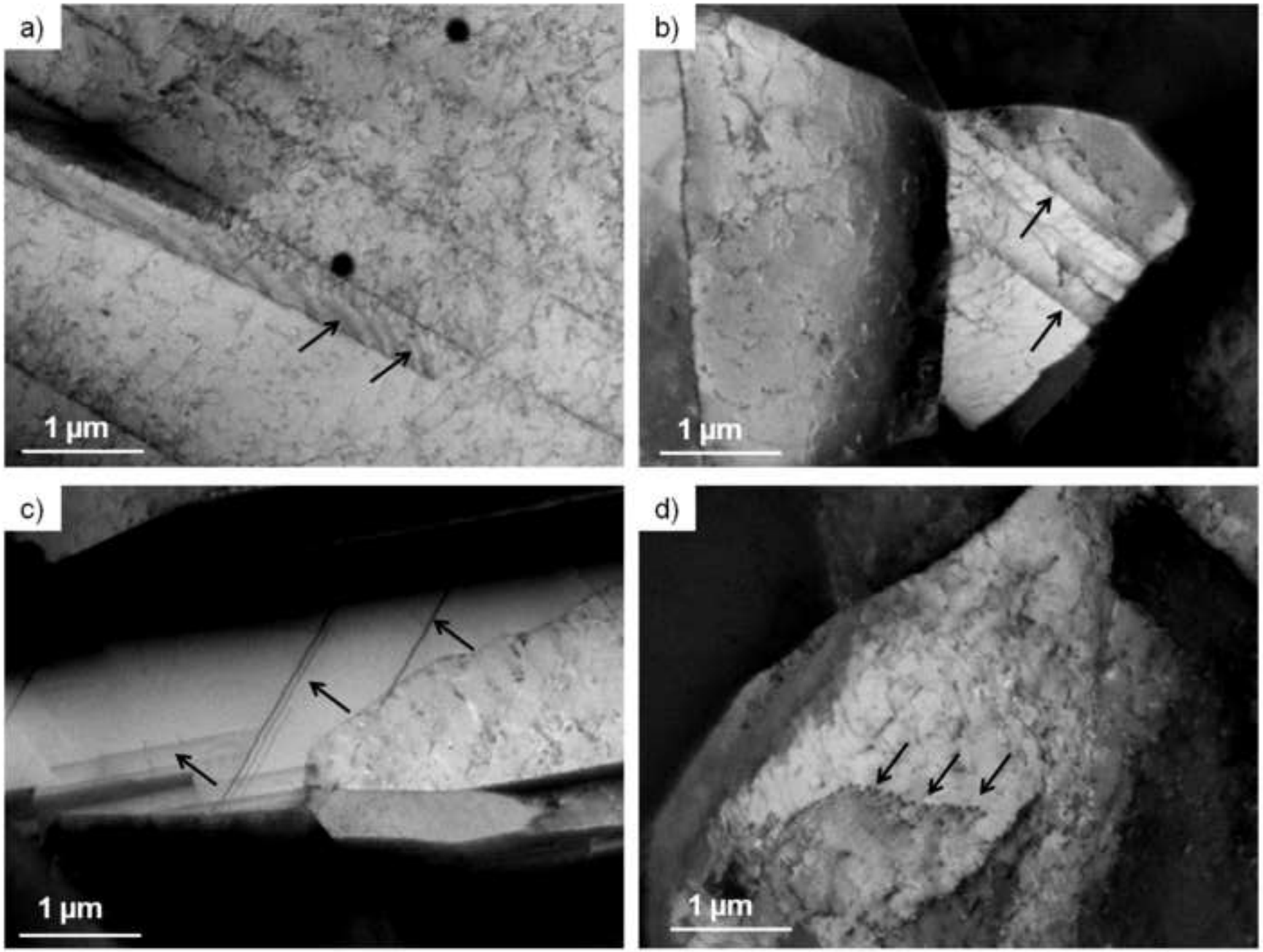

Figure_6_neu.tif
Click here to download high resolution image

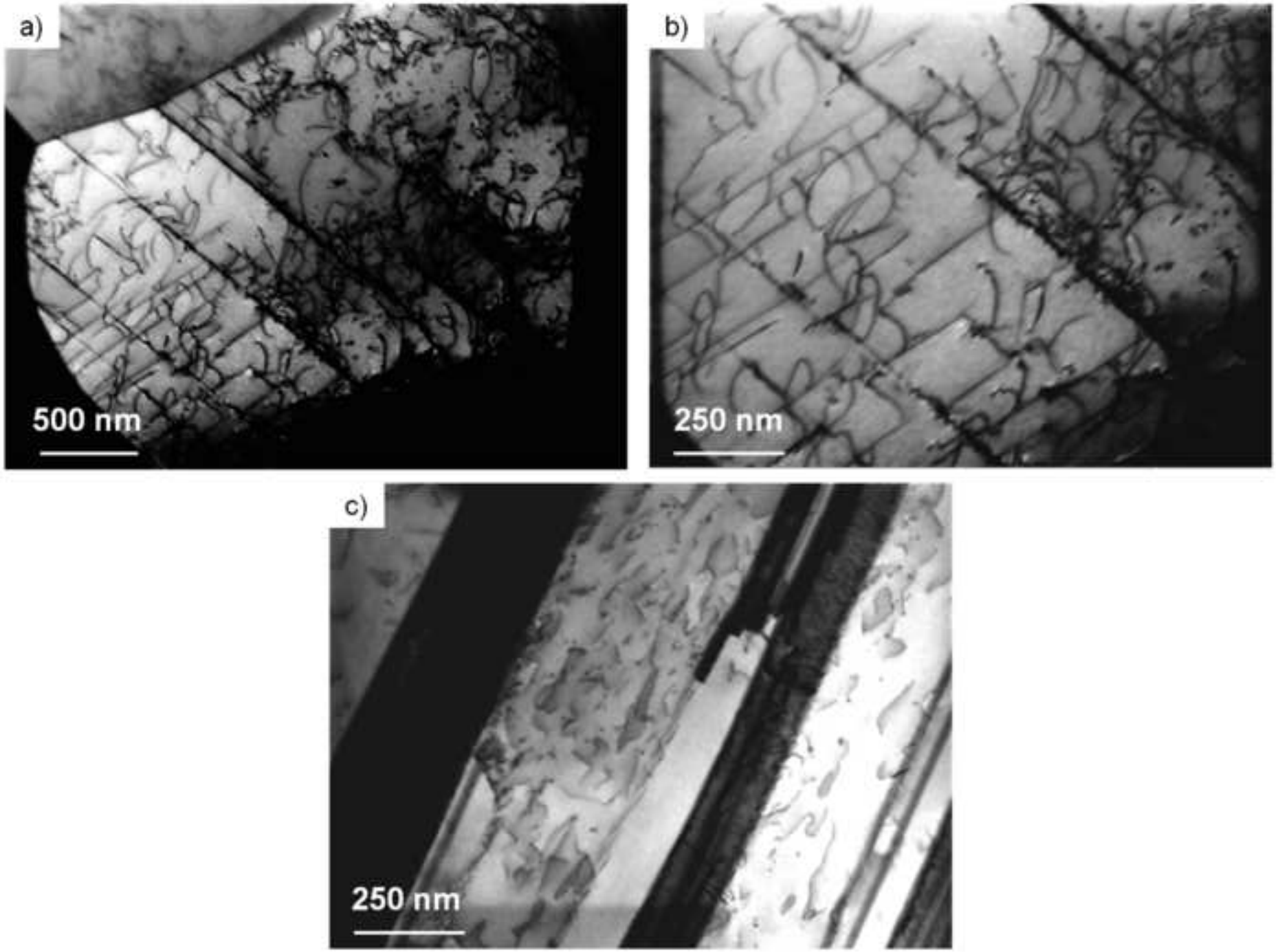

Figure_7_neu.tif
Click here to download high resolution image

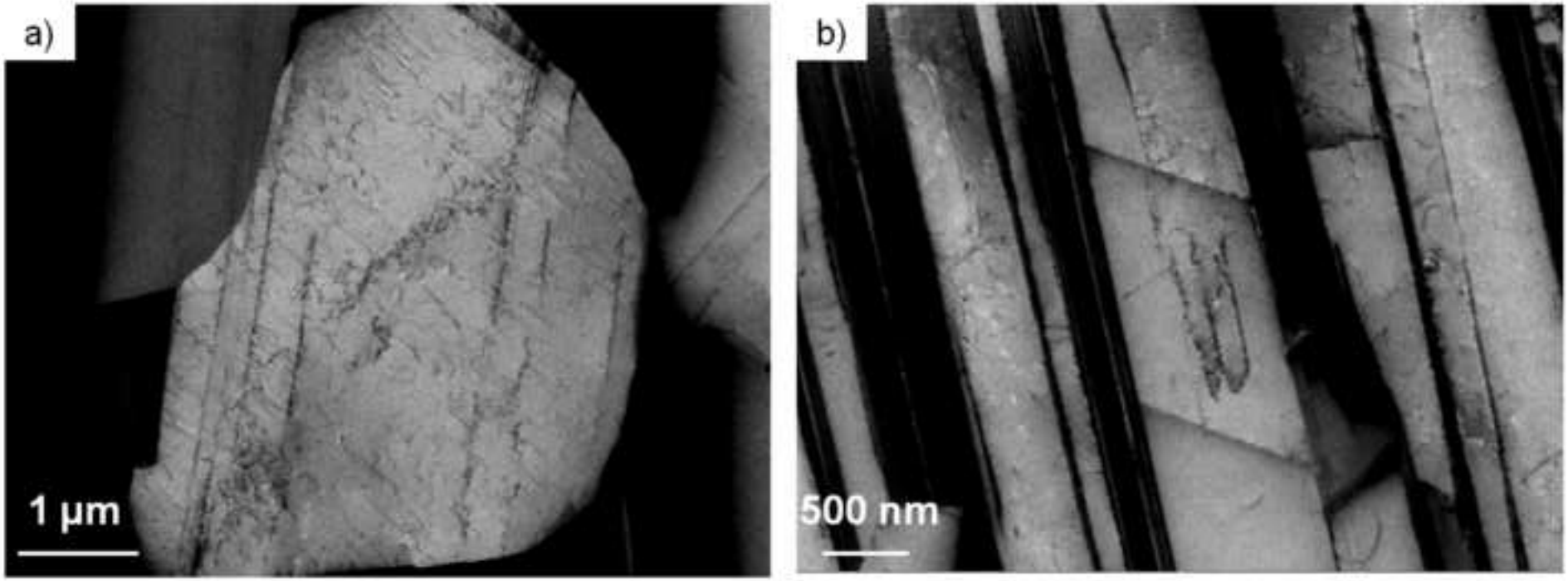

Figure_8.tif
Click here to download high resolution image

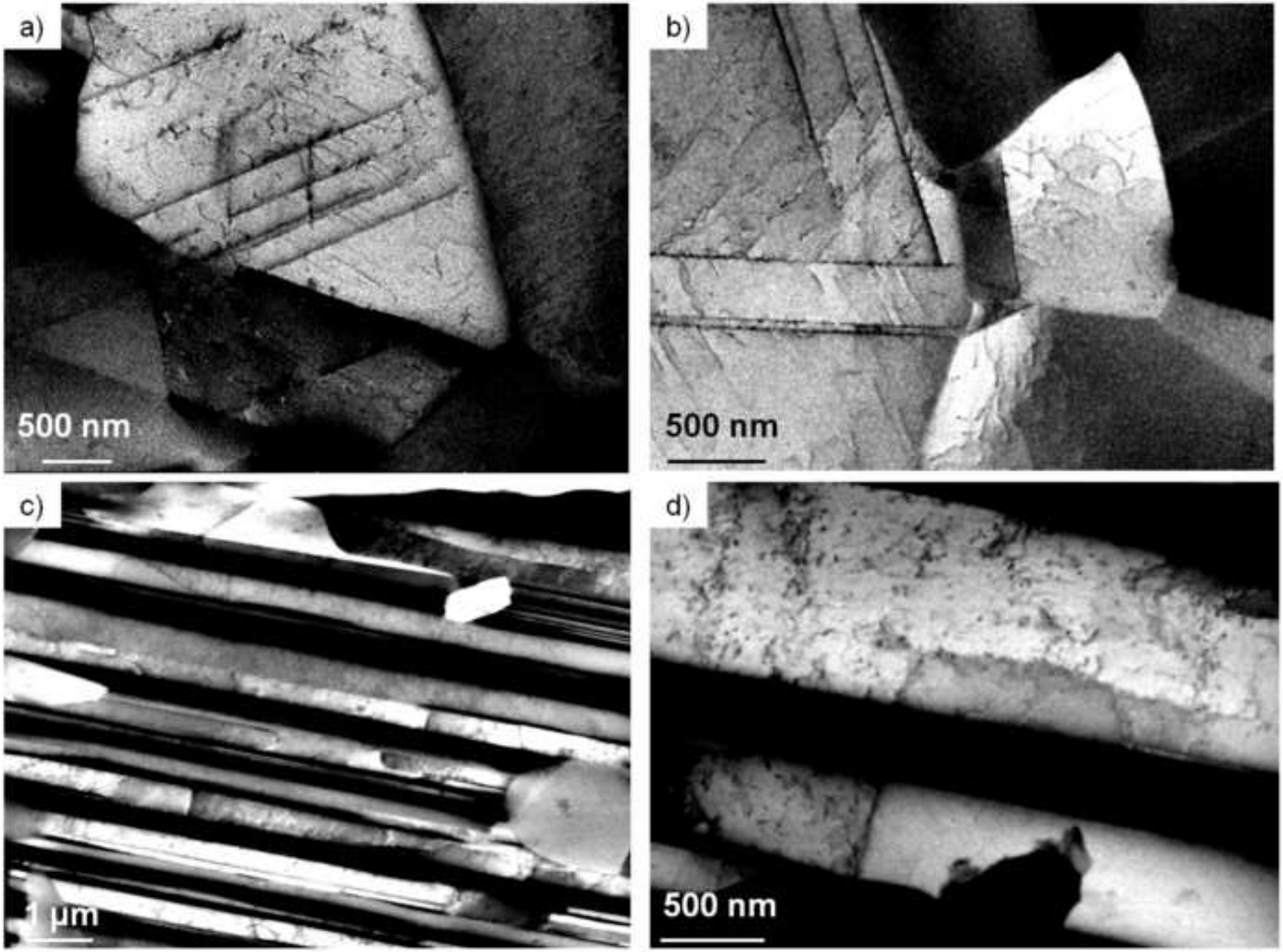

Figure_9a.tif
Click here to download high resolution image

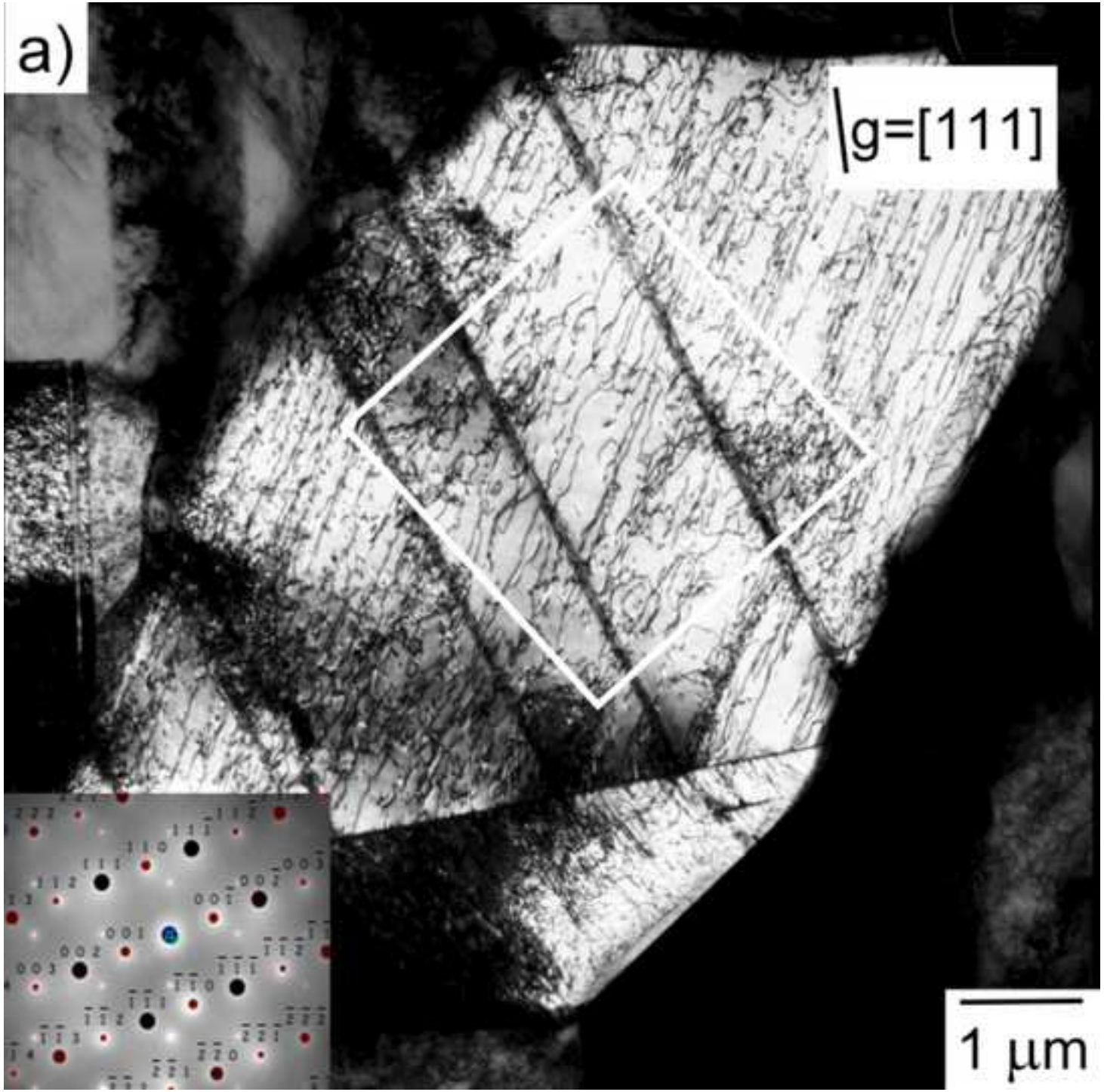

Figure_9b.tif
Click here to download high resolution image

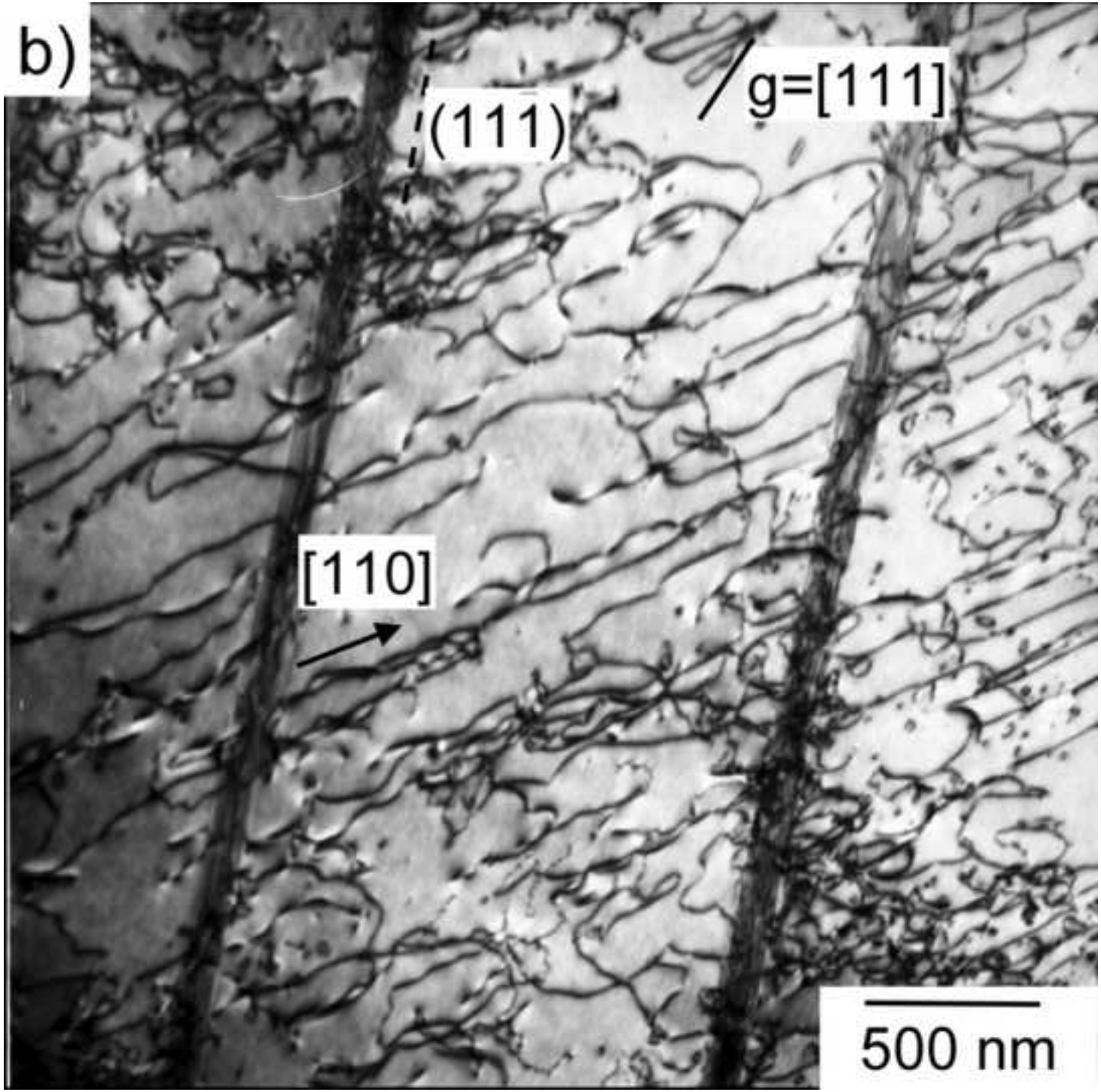

Figure_10a.tif
Click here to download high resolution image

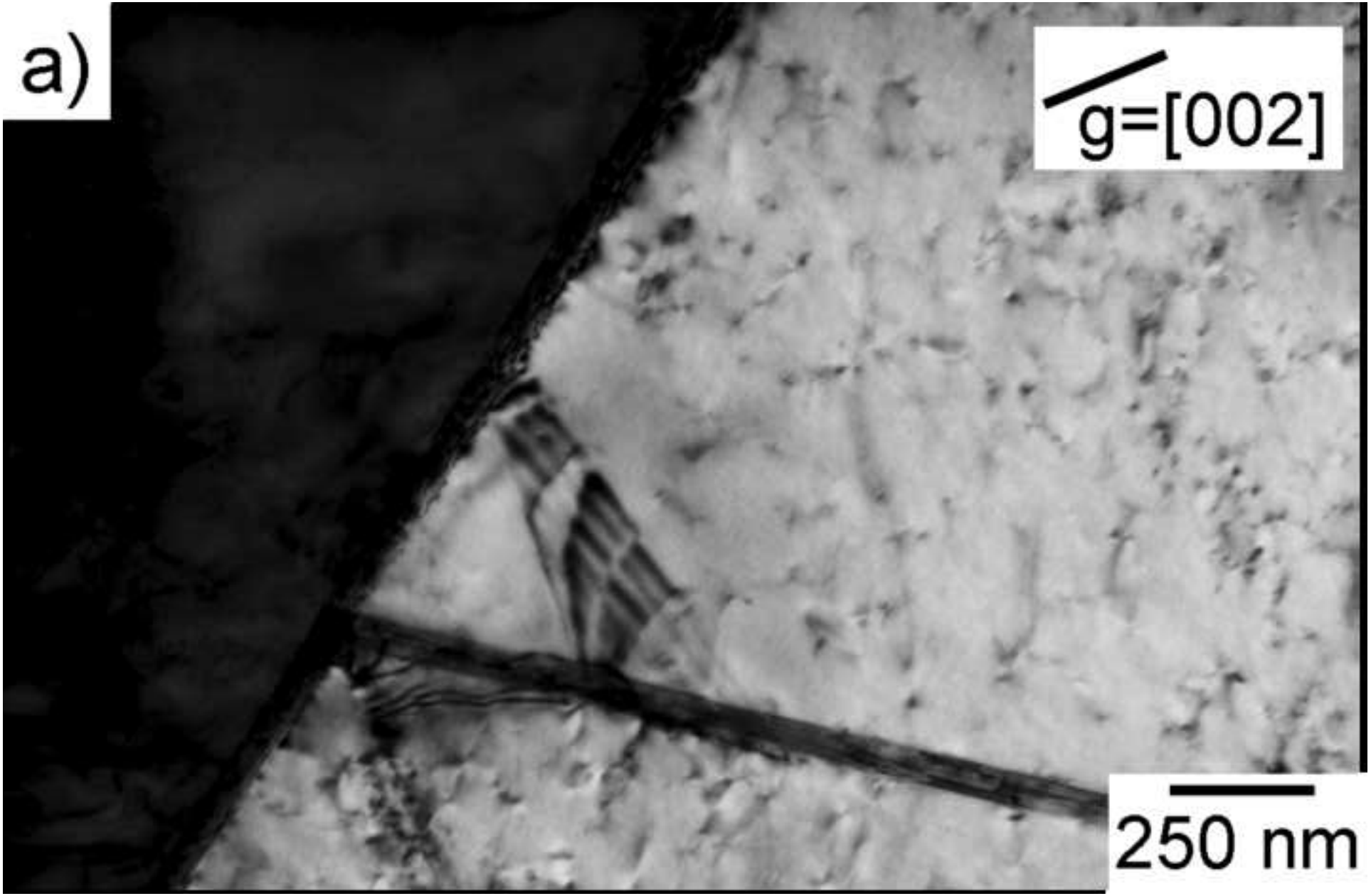

Figure_10b.tif
Click here to download high resolution image

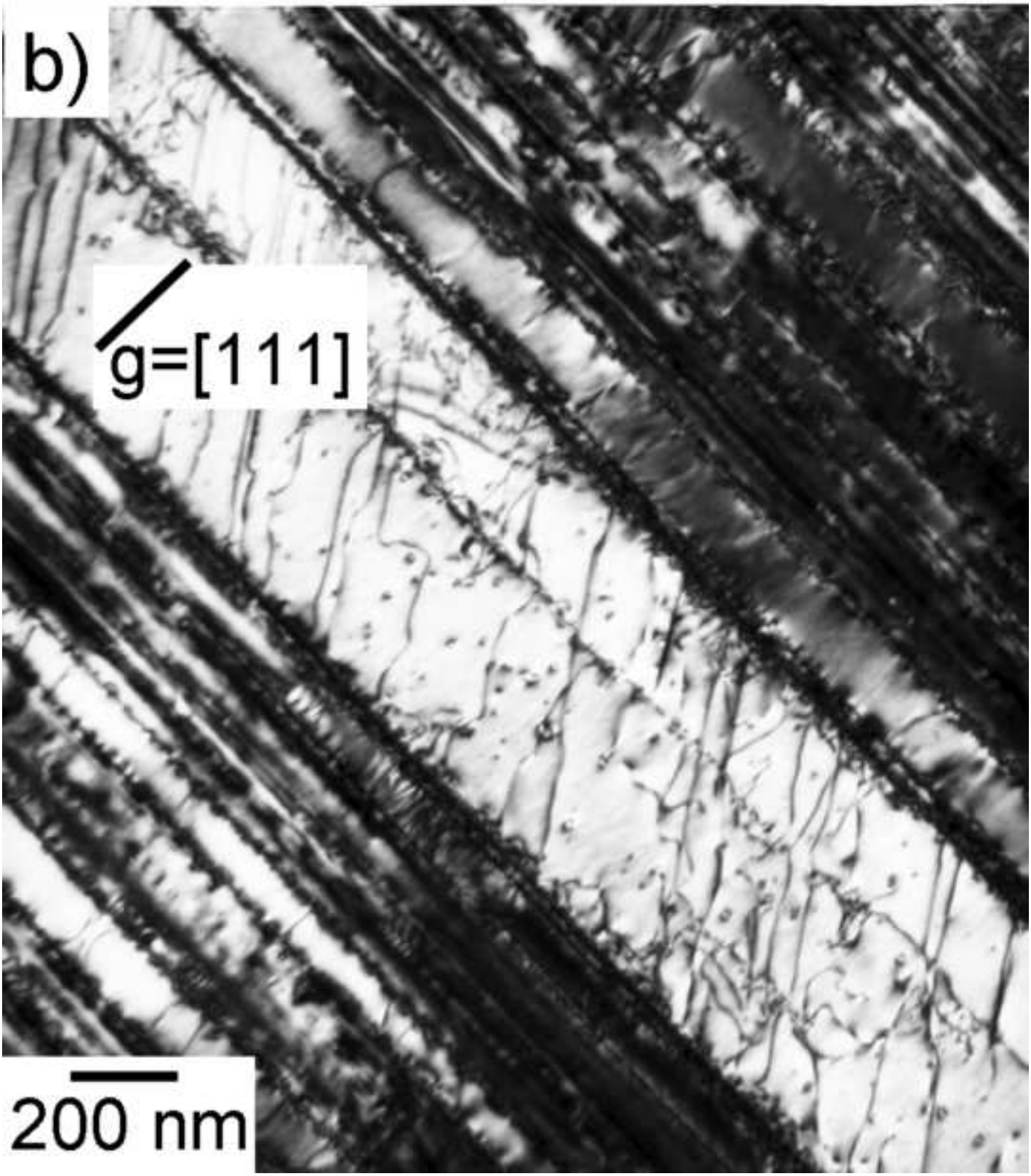

Table 1: Lattice parameters of the γ-TiAl phase and the α_2Ti_3Al-phase used for the EBSD-measurements [25].

Phase	**Length of the unit cell**			**Angles of the unit cell**			**Space group** (Hermann – Mauguin notation)
	a [nm]	**b [nm]**	**c [nm]**	**α [°]**	**β [°]**	**γ [°]**	
γTiAl	0.2837	0.2837	0.4059	90	90	90	P 4/mmm
α_2Ti_3Al	0.5764	0.5764	0.4664	90	90	120	P 63/mmc

Table_2.docx

Table 2: Crystallographic orientation given in Euler angles, g-matrix and (hkl)[uvw] for the grains labeled in Figure 3a and 3d.

	Grain number	***Euler angles***			***g-matrix***			**(hkl)**	**[uvw]**
		ϕ_1	Φ	ϕ_2					
Fig. 3a	1	2.29	0.21	4.66	0.7659 -0.6225 0.1611	0.6060 0.7826 0.1426	-0.2148 -0.0116 0.9766	(001)	[1-10]
	2	0.92	0.77	1.50	-0.5330 -0.6408 0.5526	0.4868 -0.7664 -0.4191	0.6920 0.0456 0.7204	(101)	[-1-11]
	3	2.88	2.93	5.57	-0.8956 -0.4415 0.0545	-0.4228 0.8829 0.2043	-0.1383 0.1599 -0.9774	(001)	[-2-10]
	4	3.88	1.93	0.19	-0.7689 -0.0925 -0.6326	-0.6136 0.3846 0.6896	0.1795 0.9184 -0.3525	(03-1)	[-101]
Fig. 3d	1	5.05	1.92	5.16	0.4400 0.1567 -0.8842	-0.3074 -0.8989 -0.3123	-0.8437 0.4092 -0.3473	(-21-1)	[10-2]
	2	0.76	0.77	1.43	-0.3927 -0.7841 0.4805	0.6100 -0.6131 -0.5019	0.6882 0.0960 0.7191	(101)	[-1-21]
	3	4.77	1.72	5.38	0.1536 -0.0526 -0.9867	-0.6145 -0.7871 -0.0537	-0.7738 0.6146 -0.1532	(-110)	[00-1]
	4	1.54	0.78	4.55	0.6957 0.1410 0.7044	-0.1803 0.9834 -0.0187	-0.6953 -0.1140 0.7096	(-101)	[101]